

1966

# Prediction of universal velocity distributions for fully developed turbulent flow in annuli

Daniel Kwasnoski  
*Lehigh University*

Follow this and additional works at: <https://preserve.lehigh.edu/etd>



Part of the [Chemical Engineering Commons](#)

---

## Recommended Citation

Kwasnoski, Daniel, "Prediction of universal velocity distributions for fully developed turbulent flow in annuli" (1966). *Theses and Dissertations*. 5053.  
<https://preserve.lehigh.edu/etd/5053>

This Thesis is brought to you for free and open access by Lehigh Preserve. It has been accepted for inclusion in Theses and Dissertations by an authorized administrator of Lehigh Preserve. For more information, please contact [preserve@lehigh.edu](mailto:preserve@lehigh.edu).

PREDICTION OF UNIVERSAL VELOCITY DISTRIBUTIONS  
FOR FULLY DEVELOPED TURBULENT FLOW IN ANNULI

by  
Daniel Kwasnoski

A THESIS  
Presented to the Graduate Faculty  
of Lehigh University  
in Candidacy for the Degree of  
Master of Science

Lehigh University  
1966

CERTIFICATE OF APPROVAL

This thesis is accepted and approved in partial fulfillment  
of the requirements for the degree of Master of Science.

\_\_\_\_\_  
(date)

\_\_\_\_\_  
Professor in Charge

\_\_\_\_\_  
Head of the Department

CERTIFICATE OF APPROVAL

This thesis is accepted and approved in partial fulfillment  
of the requirements for the degree of Master of Science.

---

(date)

---

Professor in Charge

---

Head of the Department

ACKNOWLEDGEMENTS

I would like to thank Professor Curtis W. Clump for his advice during the course of this investigation and Mr. F. A. Nace for typing the final draft of this paper. The suggestions and assistance of R. A. Wolfe and F. S. Patterson were also deeply appreciated. Special thanks are given to the Bethlehem Steel Corporation for making this work possible through their educational assistance program and use of their computer facilities and to my wife Carolyn who has been patient and understanding throughout the course of study.

TABLE OF CONTENTS

	Page
Title Page .....	i
Certificate of Approval .....	ii
Acknowledgements .....	iii
Table of Contents .....	iv
List of Figures .....	v
Abstract .....	1
Introduction .....	3
Analysis of Annular Flow .....	7
Development of a Diffusivity Model .....	13
Testing the Model .....	16
Discussion .....	22
Conclusions and Recommendations .....	26
List of Symbols .....	27
Graphical Comparison of Calculated and Experimental Results .....	29
Appendices .....	56
Computer Programs .....	57
Bibliography .....	63
Vita .....	66

# LIST OF FIGURES

	Page
Figure 1, Variation of Maximum Velocity Radius with Core-to-Shell Ratio of an Annulus .....	29
Figure 2, Normalized Shear Stress Distributions for Annuli with Different Core-to-Shell Ratios ...	30
Figure 3, Normalized Shear Stress Distributions for Annuli with Different Core-to-Shell Ratios ...	31
Figure 4, Universal Velocity Distributions for Air Flowing in an Annulus with a Core-to-Shell Ratio of 0.0625 at a Maximum Velocity of 30 fps .....	32
Figure 5, Universal Velocity Distributions for Air Flowing in an Annulus with a Core-to-Shell Ratio of 0.0625 at a Maximum Velocity of 60 fps .....	33
Figure 6, Universal Velocity Distributions for Air Flowing in an Annulus with a Core-to-Shell Ratio of 0.5620 at a Maximum Velocity of 30 fps .....	34
Figure 7, Universal Velocity Distributions for Air Flowing in an Annulus with a Core-to-Shell Ratio of 0.5620 at a Maximum Velocity of 60 fps .....	35
Figure 8, Mean Velocity Profiles for Air Flowing in an Annulus with a Core-to-Shell Ratio of 0.0625 at a Maximum Velocity of 30 fps .....	36
Figure 9, Mean Velocity Profiles for Air Flowing in an Annulus with a Core-to-Shell Ratio of 0.0625 at a Maximum Velocity of 60 fps .....	37
Figure 10, Mean Velocity Profiles for Air Flowing in an Annulus with a Core-to-Shell Ratio of 0.5620 at a Maximum Velocity of 30 fps .....	38

Figure 11, Mean Velocity Profiles for Air Flowing in an Annulus with a Core-to-Shell Ratio of 0.5620 at a Maximum Velocity of 60 fps .....	39
Figure 12, Universal Velocity Distributions for Air Flowing in an Annulus with a Core-to-Shell Ratio of 0.0625 at a Maximum Velocity of 30 fps .....	40
Figure 13, Universal Velocity Distributions for Air Flowing in an Annulus with a Core-to-Shell Ratio of 0.0625 at a Maximum Velocity of 60 fps .....	41
Figure 14, Universal Velocity Distributions for Air Flowing in an Annulus with a Core-to-Shell Ratio of 0.5620 at a Maximum Velocity of 30 fps .....	42
Figure 15, Universal Velocity Distributions for Air Flowing in an Annulus with a Core-to-Shell Ratio of 0.5620 at a Maximum Velocity of 60 fps .....	43
Figure 16, Mean Velocity Profiles for Air Flowing in an Annulus with a Core-to-Shell Ratio of 0.0625 at a Maximum Velocity of 30 fps .....	44
Figure 17, Mean Velocity Profiles for Air Flowing in an Annulus with a Core-to-Shell Ratio of 0.0625 at a Maximum Velocity of 60 fps .....	45
Figure 18, Mean Velocity Profiles for Air Flowing in an Annulus with a Core-to-Shell Ratio of 0.5620 at a Maximum Velocity of 30 fps .....	46
Figure 19, Mean Velocity Profiles for Air Flowing in an Annulus with a Core-to-Shell Ratio of 0.5620 at a Maximum Velocity of 60 fps .....	47
Figure 20, Universal Velocity Distributions for Air Flowing in an Annulus with a Core-to-Shell Ratio of 0.0010 at a Maximum Velocity of 30 fps .....	48



Figure 21, Universal Velocity Distributions for Air Flowing in an Annulus with a Core-to-Shell Ratio of 0.0010 at a Maximum Velocity of 60 fps .....	49
Figure 22, Universal Velocity Distributions for Air Flowing in an Annulus with a Core-to-Shell Ratio of 0.9900 at a Maximum Velocity of 30 fps .....	50
Figure 23, Universal Velocity Distributions for Air Flowing in an Annulus with a Core-to-Shell Ratio of 0.9900 at a Maximum Velocity of 60 fps .....	51
Figure 24, Mean Velocity Profile for Air Flowing in an Annulus with a Core-to-Shell Ratio of 0.0010 at a Maximum Velocity of 30 fps .....	52
Figure 25, Mean Velocity Profile for Air Flowing in an Annulus with a Core-to-Shell Ratio of 0.0010 at a Maximum Velocity of 60 fps .....	53
Figure 26, Mean Velocity Profile for Air Flowing in an Annulus with a Core-to-Shell Ratio of 0.9900 at a Maximum Velocity of 30 fps .....	54
Figure 27, Mean Velocity Profile for Air Flowing in an Annulus with a Core-to-Shell Ratio of 0.9900 at a Maximum Velocity of 60 fps .....	55

# ABSTRACT

A method was developed to predict velocity distributions for a flow system having a nonlinear stress distribution. Annuli formed by two concentric cylinders with core-to-shell ratios from 0.001 to 0.990 were investigated. The effectiveness of the method depends upon the eddy diffusivity expressions employed and an expression relating maximum velocity radius to the core-to-shell ratio of an annulus.

In this study the eddy diffusivity expressions of von Karman (25) were used although those of Prandtl (9) or others could also have been applied. Two schemes for relating maximum velocity radius to core-to-shell ratio of an annulus were tested. These schemes were selected because they represent the extremes of published experimental data. The first assumes that the laminar and turbulent maximum velocity radii are identical. The second is based on experimental data of Brighton and Jones (3) that cover a broad range of annuli core-to-shell ratios.

The IBM 1620 digital computer was used to develop a diffusivity model that is essentially a systematic application of the method developed herein. The only information needed to predict velocity distributions for turbulent annular flow when the model is employed is as follows:

1. Core radius of annulus, ft

2. Shell radius of annulus, ft
3. Maximum velocity flow, ft/sec, and
4. Kinematic viscosity of the fluid,  $\text{ft}^2/\text{sec}$ .

Comparisons of distributions calculated by the model with the experimental data of Brighton and Jones (3), Knudsen and Katz (11), Sparrow et.al. (24), and Okiishi et.al. (16) show that good agreement between calculated and measured values can be obtained over a broad range of annuli core-to-shell ratios. In addition, the model includes, in part, the effect of Reynold's number on velocity distribution, an effect recognized by other investigators (10).

### INTRODUCTION

Fully developed turbulent flow of a Newtonian incompressible fluid in annuli is of interest to the engineer because of its direct engineering applications and to the scientist because it can provide insight into the problem of developing a complete theory of turbulent flow. The two limiting cases of one-dimensional fully developed turbulent flow in annuli have been studied in detail. They are: flow in circular pipes and flow between parallel flat plates. For flows of these types the velocity distributions can be predicted within the accuracy of experimental data by using various universal velocity distribution laws (6,17,23,25). Although Hinze (10) points out that better predictions would be obtained if the laws were modified to include the effect of Reynold's number, their utility is evident from their widespread engineering applications to flow in pipes and between parallel flat plates.

For flow in annuli the predictions obtained from the universal velocity distribution laws are in obvious disagreement with experimental data (3,11). This discrepancy arises for two reasons. First, fully developed annular flow exists within two regions, each extending from a wall to a point of maximum velocity. Unlike the case of flow through pipes and flow between parallel plates where the point of maximum velocity is midway between opposing walls, for annular flow the point of maximum velocity lies nearer the core wall. Second the shear stress is

not a linear function of distance from the wall, particularly for annuli with small core-to-shell ratios. For flow through pipes and flow between parallel flat plates the shear stress distributions are essentially linear.

Sparrow et.al. (24) acknowledged the presence of a nonlinear stress distribution in a study of flow longitudinal to a cylinder. They applied a stress distribution of the form<sup>a</sup>

$$\frac{\tau}{\tau_w} = \frac{r}{r+y} \quad (1)$$

to the shear stress-eddy diffusivity relationship

$$\frac{\tau}{\tau_w} = \frac{(1+\epsilon)}{v} \frac{du^+}{dy^+} \quad (2)$$

and determined universal velocity distributions by numerically integrating the expression

$$\frac{du^+}{dy^+} = \frac{vr}{(1+\epsilon)(r+y)} \quad (3)$$

Wolffe (28,29) proposed that this method be extended to study flow in annuli in which the shear stress distributions can be rigorously calculated from a simple force balance when the maximum velocity radius is known. The modified  $u^+$   $y^+$  relationships obtained could be compared with experimental data and universal velocity distribution law predictions to determine the applicability of diffusivity models. This is the purpose of the present study.

---

<sup>a</sup> A complete list of symbol definitions is given on page 27.

Before attempting to derive new universal velocity relations based on a diffusivity model it is best to comment on the findings of other investigators in this field. The exact location of the maximum velocity for turbulent annular flow, which is needed to calculate the shear stress distributions used in a diffusivity model, is under disagreement. Rothfus (19) and Knudsen and Katz (11) concluded that the location of the maximum velocity for turbulent flow was "essentially" the same as for laminar flow. More recent work by Brighton and Jones (3) suggests that the maximum velocity radii for turbulent flow in annuli are different from those for laminar flow with the location being a function of the Reynold's number and the core-to-shell ratio of the annulus.

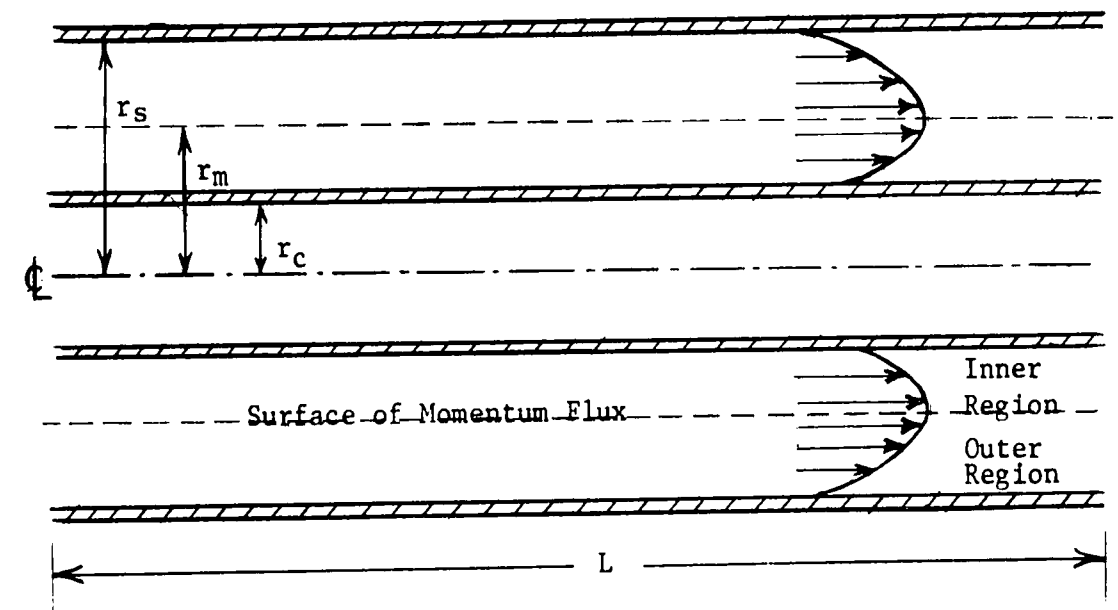
The relationship between eddy diffusivity and velocity gradient is also subject to disagreement. The purely phenomenological eddy diffusivity expressions of von Karman (25) and others (9) have been criticized because in many instances the assumed mechanics of turbulent transport have been experimentally proven to be incorrect. In spite of these shortcomings the phenomenological models have not been replaced to any great extent by current efforts to describe the actual turbulent transport mechanism. Still, there are many phenomenological eddy diffusivity expressions (9) which could be used to develop a model and the problem remains of deciding which one to use.

For this study, the eddy diffusivity-velocity gradient equations derived by Deissler (6) from von Karman's diffusivity expressions were employed. Because of the obvious disagreement in the location of the maximum velocity radius, the study was repeated for two cases:

1. The laminar and turbulent maximum velocity radii are assumed identical as proposed by Rothfus (19) and Knudsen and Katz (11), and
2. An expression based on the experimental data of Brighton and Jones (3) to locate the maximum velocity radius is employed.

# ANALYSIS OF ANNULAR FLOW

The stress distribution functions for flow in an annulus can be obtained from simple force balances. These balances are written across two flow regions, one bounded by the shell and the maximum velocity radius and the other by the maximum velocity radius and the core.



Consider the balance between pressure loss and shear stress for an element  $L$  units long bounded by the maximum velocity radius,  $r_m$ , and some radius larger than  $r_m$  but smaller than the shell radius,  $r_s$ .

$$\frac{dP}{dL} (r^2 - r_m^2) \pi L = \tau 2\pi r L \quad (4)$$



If this expression is divided by the balance written for the region between  $r_m$  and  $r_s$

$$\frac{dP}{dL} (r_s^2 - r_m^2) \pi L = \tau_s 2 \pi r_s L \quad (5)$$

where the shear stress will be the stress at the wall, the resulting expression is the shear stress distribution for the region bounded by the maximum velocity radius and the shell wall of the annulus.

$$\frac{\tau}{\tau_s} = \frac{(r_m^2 - r_s)}{(r_m^2 - r_s^2)} \left\{ \frac{1}{r} - \frac{r}{r_m^2} \right\}; r_s > r > r_m \quad (6a)$$

Similarly, for the region bounded by the maximum velocity radius and the core wall of the annulus, the shear stress distribution is given by.

$$\frac{\tau}{\tau_c} = \frac{(r_m^2 - r_c)}{(r_m^2 - r_c^2)} \left\{ \frac{1}{r} - \frac{r}{r_m^2} \right\}; r_m > r > r_c \quad (6b)$$

It should be noted that these balances are based on the assumption that no shear stress exists when the velocity gradient is zero, i.e., at the point of maximum velocity.

Equations 6a and 6b can be used to calculate the shear stress distribution for any annulus when the maximum velocity radius is known. In this study two methods for determining the maximum velocity radius will be evaluated. These methods were selected because they represent the extremes of published experimental data. The first is based on the assumption that

the laminar and turbulent maximum velocity radii are identical and are given by (2).

$$r_m = r_s \left\{ \frac{1 - (\alpha)^2}{2 \ln(1/\alpha)} \right\}^{1/2} \quad (7)$$

The second method for determining the maximum velocity radius is based on equations obtained from the experimental data of Brighton and Jones using standard polynomial curve-fitting techniques (21). Although the data indicate a slight Reynold's number effect at low core-to-shell ratios, it was excluded from the present work. The expressions obtained relate the maximum velocity radius to core-to-shell ratio as follows:

$$r_m = r_c + \left\{ \frac{(r_s - r_c)}{2} [1.075\alpha^3 - 2.203\alpha^2 + 1.652\alpha + .475] \right\} \quad (8)$$

for  $.0625 < \alpha < 1.0$ , and

$$r_m = r_c + \left\{ \frac{(r_s - r_c)}{2} \frac{(.5650)}{(.0624)} \right\} \alpha \quad (9)$$

for  $0 < \alpha < .0625$

A comparison of the maximum velocity radii calculated using equation 7 and equations 8 and 9 over a broad range of annuli core-to-shell ratios is presented in Figure 1. Figure 2 shows the effect of core-to-shell ratio on shear stress distribution for concentric annuli when equations 6a, 6b, and 7 are used. Figure 3 shows the effect when equations 8 and 9 are combined with equations 6a and 6b.

Employing the definition of eddy diffusivity a simple stress equation can be written.

$$\tau = (\mu + \epsilon) \frac{du}{dy} \quad (10)$$

Equation 10 can be combined with equations 6a and 6b to derive the expressions describing the velocity distributions for the outer and inner regions of an annulus.

$$\frac{du_o}{dy_o} = \left\{ \frac{\tau_s}{\mu + \rho\epsilon} \right\} \left\{ \frac{r_m^2 r_s}{(r_m^2 - r_s^2)} \left[ \frac{1}{r} - \frac{r}{r_m^2} \right] \right\} \quad (11a)$$

$$\frac{du_i}{dy_i} = \left\{ \frac{\tau_c}{\mu + \rho\epsilon} \right\} \left\{ \frac{r_m^2 r_c}{(r_m^2 - r_c^2)} \left[ \frac{1}{r} - \frac{r}{r_m^2} \right] \right\} \quad (11b)$$

By applying the definitions of  $y$ ,  $u^+$ , and  $y^+$  for the two regions

$$y_o = r_s - r \quad (12a)$$

$$y_i = r - r_c \quad (12b)$$

$$u_o^+ = u_o / u_o^* \quad (13a)$$

$$u_i^+ = u_i / u_i^* \quad (13b)$$

$$y_o^+ = (y_o u_o^*) / \nu \quad (14a)$$

$$y_i^+ = (y_i u_i^*) / \nu \quad (14b)$$

the shear stresses at the boundaries,  $\tau_s$ , and  $\tau_c$ , can be deleted from equations 11a and 11b to yield expressions describing the universal velocity distributions for the two regions.

$$\frac{du_o^+}{dy_o^+} = \left\{ \frac{r_m^2 r_s}{(r_m^2 - r_s^2)(1 + \epsilon/v)} \right\} \left\{ \left[ \frac{u_o^*}{u_o^* r_s - y_o^+ v} \right] - \left[ \frac{u_o^* r_s - y_o^+ v}{u_o^* r_m^2} \right] \right\} \quad (15a)$$

$$\frac{du_i^+}{dy_i^+} = \left\{ \frac{r_m^2 r_c}{(r_m^2 - r_c^2)(1 + \epsilon/v)} \right\} \left\{ \left[ \frac{u_i^*}{u_i^* r_c + y_i^+ v} \right] - \left[ \frac{u_i^* r_c + y_i^+ v}{u_i^* r_m^2} \right] \right\} \quad (15b)$$

To solve these expressions a relationship between eddy diffusivity and velocity gradient is required. Deissler (6) derived two convenient expressions from von Karman's diffusivity expressions.

$$\epsilon/v = n^2 u^+ y^+ ; y^+ < 26 \quad (16)$$

$$\epsilon/v = K^2 (du^+/dy^+)^3 / (d^2 u/dy^+)^2 ; y^+ > 26 \quad (17)$$

If these expressions are employed four differential expressions result which describe the annular flow conditions.

for  $y^+ < 26$ , across the outer region

$$\frac{du_o^+}{dy_o^+} = \left\{ \frac{r_m^2 r_s}{(r_m^2 - r_s^2)(1 + n^2 u_o^+ y_o^+)} \right\} \left\{ \left[ \frac{u_o^*}{u_o^* r_s - y_o^+ v} \right] - \left[ \frac{u_o^* r_s - y_o^+ v}{u_o^* r_m^2} \right] \right\} \quad (18a)$$

for  $y^+ < 26$ , across the inner region

$$\frac{du_i^+}{dy_i^+} = \left\{ \frac{r_m^2 r_c}{(r_m^2 - r_c^2)(1 + n^2 u_i^+ y_i^+)} \right\} \left\{ \left[ \frac{u_i^*}{u_i^* r_c + y_i^+ v} \right] - \left[ \frac{u_i^* r_c + y_i^+ v}{u_i^* r_m^2} \right] \right\} \quad (18b)$$

for  $y^+ > 26$  across the outer region

$$\frac{du_o^+}{dy_o^+} = \frac{K (du_o^+/dy_o^+)^2}{\left\{ \frac{r_m^2 r_s}{(r_m^2 - r_s^2)(1 + n^2 u_o^+ y_o^+)} \right\} \left\{ \left[ \frac{u_o^*}{u_o^* r_s - y_o^+ v} \right] - \left[ \frac{u_o^* r_s - y_o^+ v}{u_o^* r_m^2} \right] \right\} - \frac{du_o^+}{dy_o^+}}^{1/2} \quad (19a)$$

for  $y^+ > 26$  across the inner region

$$\frac{du_1^+}{dy_1^+} = \frac{K(du_1^+/dy_1^+)^2}{\left\{ \frac{[r_m^2 r_c]}{[r_m^2 - r_c^2]} \left[ \left( \frac{u_1^*}{(u_1^* r_c + y_1 + v)} - \frac{(u_1^* r_c + y_1 + v)}{(u_1^* r_m^2)} \right) - \frac{du_1^+}{dy_1^+} \right] \right\}^{1/2}} \quad (19b)$$

Successful integration of these equations results in curves of  $u^+$  vs.  $y^+$  for the two regions of flow.

# DEVELOPMENT OF A DIFFUSIVITY MODEL

The model developed here is essentially a systematic method of solving the differential universal velocity distribution equations (Eqns. 18a, 18b, 19a, and 19b) derived in the previous section. Numerical techniques are available to integrate equations of these types (21); but the limits of integration must be firmly defined. For equations 18a and 18b no problem exists since the limits are set, by definition, at  $y^+ = 0$  and  $y^+ = 26$ . For 19a and 19b, however, the expressions must be integrated from  $y^+ = 26$  to some as yet undetermined value of  $y^+$  where the velocity is a maximum. This problem can be resolved by observing that at  $y^+ = y_m^+$ , the following relationship must also be satisfied.

$$u_m^+ = (u_m y_m) / (y_m^+ \nu) \quad (20)$$

A trial and error approach can then be used to solve equations 18a through 19b within any desired accuracy. In this study the following procedure was used:

1. Assume a value for  $u_m^+$ , the maximum value of  $u^+$ ,  
i.e., the value of  $u^+$  at  $y_m^+$ .

2. Calculate  $u^*$  from the expression

$$u^* = u_m / u_m^+ \quad (21)$$

3. Calculate  $y_m^+$  from the relationship

$$y_m^+ = u^* y_m / \nu \quad (22)$$

4. Integrate equation 18a from  $y^+ = 0$  to  $y^+ = 26$  using a standard numerical method for solving equations of the first order.
5. Integrate equation 19a from  $y^+ = 26$  to  $y^+ = y_m^+$  using a standard numerical method for solving equations of the second order.
6. Compare the value of  $u_m^+$  obtained from the integration with the assumed value of Step 1.
7. Modify the assumed value of  $u_m^+$  and repeat Steps 1 through 6 until the desired agreement is reached between the assumed and calculated values of  $u_m^+$ .
8. Repeat Steps 1 through 7 for the integration of equations 18b and 19b.

To facilitate the calculations this trial and error procedure was programmed for the IBM 1620 digital computer. The expressions, 18a and 18b were solved using the modified Euler method because derivatives of the first order only are involved. To start this method the initial conditions of  $u^+ = 0$  and  $du^+/dy^+ = 1$  at  $y^+ = 0$  are used. The integration then proceeds in  $y^+$  increments calculating and correcting  $u^+$  for each forward step. Only two points are needed for each calculation, the previous point and the new point. The value of  $u^+$  at the new point is first calculated using the slope at the old point and an increment distance in the  $y^+$  direction. For

each point the procedure was repeated until the change in  $u^+$  for the new point was less than 0.001. It was found that tests with increments from 0.1 to 0.5 produced essentially no change in the  $u^+$   $y^+$  distribution and a value of 0.5 was deemed satisfactory for subsequent integrations.

To integrate equations 19a and 19b the second order Runge-Kutta method was used. This method is not iterative. A single solution is obtained by applying the set of formulae of Runge and Kutta (21). Tests of this method with increment sizes from 0.1 to 0.5 again showed essentially no change in the  $u^+$   $y^+$  distributions obtained and a value of 0.5 was selected for the balance of the integrations.

The following information is all that is needed when using the model to predict the velocity distribution for flow in an annulus:

1. Core radius of annulus, ft.
2. Shell radius of annulus, ft.
3. Maximum velocity flow, ft/sec.
4. Kinematic viscosity of the fluid,  $\text{ft}^2/\text{sec}$ .

Because the shear stresses at the walls of the annulus are calculated using a model of this type, universal velocity distributions are readily converted to mean velocity profiles. Additional information, such as velocity gradients and average velocities, can also be computed with a minimum amount of effort, or in the case of computer application, with a slight increase in machine time. A copy of the computer program used to test the model is presented in the Appendix.



TESTING THE MODEL

The model was initially tested using the assumption that the laminar and turbulent maximum velocity radii are identical and satisfy the relationship shown in Equation 7. Values of  $n = 0.109$  and  $K = 0.48$  were selected for the coefficients appearing in the diffusivity expressions (equations 16 and 17) of Deissler. These values were employed by Wolfe (28, 29) in earlier work and were deemed satisfactory for preliminary testing. The differential universal velocity distribution equations (18a, 18b, 19a and 19b) were then solved for annuli with 8 inch shells and 0.5 inch and 4.5 inch cores, or core-to-shell ratios of 0.0625 and 0.562, respectively. Calculations were performed for air flowing at maximum velocities of 30 and 60 feet per second. These conditions were employed by Brighton and Jones (3) in their experimental work and their application afforded a direct comparison between calculated and experimental results.

Universal velocity distributions predicted by the model were then compared with the experimental data of Brighton and Jones, as well as with velocity distributions predicted by two of the published universal velocity distribution laws. The distributions predicted by the model showed some improvement over those predicted by the universal velocity distribution laws but were in poor agreement with

experimental results. This was particularly evident for the annulus having the smaller core-to-shell ratio. Trials were repeated using different values for the constants  $n$  and  $K$  in the diffusivity expressions but no further improvement could be shown. In general, when better agreement was obtained for the velocity distribution of the inner region, it was done at the expense of the distribution for the outer region.

An attempt was made to correct this discrepancy by using variables for the coefficients  $n$  and  $K$  appearing in Deissler's diffusivity expressions (equations 16 and 17). The coefficient  $n$  in the expression for  $y^+ < 26$  was replaced with the expression

$$n = a + \left\{ \frac{b y^+}{26} \frac{(r_s - r_c)}{y} \right\} \quad (23)$$

and for  $y^+ > 26$  the expression

$$K = c + \left\{ \frac{26d}{y^+} \frac{(r_s - r_c)}{y} \right\} \quad (24)$$

was used. These expressions were assumed somewhat arbitrarily in an attempt to better fit the model to the experimental data. The calculations were repeated for the two core-to-shell ratios and the two maximum velocity flow conditions previously discussed. The best fit of predicted distributions with experimental data was obtained with  $a = 0.109$ ,  $b = 0.010$ ,  $c = 0.360$ , and  $d = 0.20$ . Results are presented in Figures 4-7. As shown in these figures,

the model could be used to predict universal velocity distributions over a reasonable range of annuli core-to-shell ratios.

The next test was designed to convert the universal velocity distributions to their corresponding mean velocity profiles for further comparison with experimental data. As discussed earlier, this can be done by employing equations 13a, 13b, 14a, and 14b at the maximum values of  $u^+$  and  $y^+$ , which are now known, to calculate the shear stresses at the shell and core walls. Upon substitution of these values back into the equations, direct relationships are obtained between the mean and universal velocity distributions. This procedure was used to convert the universal velocity distributions that were predicted by the model and presented in Figures 4-7. The corresponding mean velocity profiles are compared with the experimental data of Brighton and Jones in Figures 8-11, respectively. As shown in these figures, the fit between calculated and experimental results is not good. This is due, primarily to the difference in the location of the maximum velocity radii.

At this stage it was decided to repeat the study using Equations 8 and 9, which were based on experimental data, to determine the maximum velocity radii. This was done, first using constants for the coefficients  $n$  and  $K$  in Deissler's diffusivity expressions. Numerous tests were made assigning different sets of values to these coefficients but no improvement could be shown. Equations 23 and 24 were then employed as before to replace the constant values for the

coefficients with variables which are a function of  $u^+$ ,  $y^+$ , and the geometry of the annulus. Again, after repeated tests to study a broad range of values for the constants  $a$ ,  $b$ ,  $c$ , and  $d$  which appear in these equations, no better fit could be attained between calculated and experimental results. In fact, the  $u^+$   $y^+$  distributions obtained were not as good as those which appear in Figures 4-7. It was observed that when Equations 8 and 9 were used to determine the maximum velocity radii the model failed to produce the marked distinction between the universal velocity distributions for the inner and outer regions. It was decided to employ expressions for the coefficients  $n$  and  $K$  which would have a more pronounced effect on the difference between the flow conditions of these two regions, particularly for annuli with smaller core-to-shell ratios. For the outer region the equations had the form

$$n = f + \left\{ \frac{gy^+}{26} \frac{(r_m - r_c)}{(r_s - r_m)} \right\} ; 0 < y^+ < 26 \quad (25a)$$

and

$$K = h + \left\{ \frac{20j}{y^+} \frac{(r_m - r_c)}{(r_s - r_m)} \right\} ; 26 < y^+ < y_m^+ \quad (26a)$$

For the inner region the equations used were

$$n = f + \left\{ \frac{gy^+}{26} \frac{(r_s - r_m)}{(r_m - r_c)} \right\} ; 0 < y^+ < 26 \quad (25b)$$

and

$$K = h + \left\{ \frac{20j}{y^+} \frac{(r_s - r_m)}{(r_m - r_c)} \right\} ; 26 < y^+ < y_m^+ \quad (26b)$$

When these expressions were incorporated into the model good agreement was reached between calculated experimental and universal velocity distributions. The best fit was obtained when the values  $f = 0.109$ ,  $g = 0.010$ ,  $h = 0.360$ , and  $j = 0.200$  were assigned to the constants appearing in expressions 25a through 26b. Comparative results are presented in Figures 12-15. As was done in earlier testing, the universal velocity distributions were converted to their corresponding mean velocity profiles for further comparison with experimental data. The mean velocity profiles obtained from the universal distributions shown in Figures 12-15 are given in Figures 16-19 respectively. As shown in these figures, good agreement was reached between calculated and experimental results for annuli with significantly different core-to-shell ratios. In addition, the model showed a Reynold's number effect between maximum velocity flows of 30 and 60 feet per second. The experimental data presented, as well as other data compared on a qualitative basis, also showed an effect of this type.

A final test of the model at the extreme conditions of an annulus having a very small core-to-shell ratio (approaching tube flow) and a very large core-to-shell ratio (approaching flow between parallel flat plates) was considered necessary. This test was made employing core-to-shell ratios of 0.001 and 0.99, and maximum velocities of 30 and 60 feet per second. Results obtained for the universal velocity distributions are presented in Figure 16-19, and the corresponding mean velocity profiles are presented in

Figures 20-23. As shown in these figures, the model produces the velocity distributions expected at these conditions.

### DISCUSSION

An eddy diffusivity model was developed which can be used to predict velocity distributions for turbulent flow in annuli. Comparison of distributions calculated by the model with experimental data of Brighton and Jones (3), Knudsen and Katz (11), and Sparrow, Eckert and Minkowycz (24) shows that good agreement between calculated and measured values can be attained over a broad range of annuli core-to-shell ratios. In addition, the model includes the effect of Reynold's number on velocity distribution. This effect was recognized by Hinze (10) who suggested that the universal velocity distribution laws be modified to consider it.

It is believed that the significant advantage of using a diffusivity model to predict velocity distributions lies in the inherent ability to consider systems with nonlinear stress distributions. (Experimental measurements of mean velocities in turbulent flow past solid boundaries show that when the shear stress is not a linear function of distance from the solid boundary, the universal velocity distribution laws fail to predict the actual velocity distribution). To employ the diffusivity concept to a given system, the nonlinear stress distributions must either be known or readily calculable. For the case of annular flow considered in this study, simple force balances were employed to calculate these distributions. Unfortunately, a shortcoming in the

theory of turbulent flow made it necessary to rely on assumptions or experimental data to determine the maximum velocity radius on which the results of the force balances rely.

Because the theoretical maximum velocity radii can be calculated for laminar annular flow, tests were made to check out the theory of Rothfus (19) and Knudsen and Katz (11) that the laminar and turbulent maximum velocity radii are identical. Throughout these tests the coefficients in the equations which comprise the model were varied until the best fit between calculated and experimental results was obtained. The results of these tests, some of which are presented in Figures 4-11, show that agreement could not be reached between calculated and experimental results over a broad range of core-to-shell ratios.

Experimental data of Brighton and Jones (3) were then used to generate equations 8 and 9 which show the turbulent flow maximum velocity radius as a function of annulus core-to-shell ratio. Their data also showed a slight effect of Reynold's number on maximum velocity radius at small core-to-shell ratios but it was excluded from this work. Tests were again made to determine how well calculated and experimental results compared. As shown in Figures 12-19, good agreement was reached at two flow rates and over a wide range of annulus core-to-shell ratios when calculated results and the experimental data of Brighton and Jones (3) were compared. Good agreement was also found when the calculated



results were compared with experimental data of Sparrow, Eckert and Minkowycz (24) and Knudsen and Katz (11).

In the development of the model the expressions used to relate eddy diffusivity and velocity gradient were those derived by Deissler from von Karman's diffusivity expressions. It should be noted that the method employed here is not limited to the application of these particular expressions. In fact, if further work is done in this area it is recommended that other diffusivity expressions should be tried.

The following information is all that is required to predict universal velocity distributions for turbulent annular flow when the diffusivity model is employed:

1. Core radius of annulus, ft
2. Shell radius of annulus, ft
3. Maximum velocity flow, ft/sec, and
4. Kinematic viscosity of the fluid,  $\text{ft}^2/\text{sec}$ .

A trial and error technique was developed in which this minimal information can be used to obtain exact solutions to the differential universal velocity distribution equations developed through the eddy diffusivity concept (see equations 18a-19b). It was then shown how these solutions could be used to calculate the shear stresses at the core and shell walls and the mean velocity profiles. It follows that the average velocity can also be readily calculated, and herein lies the utility of the method.

For example, a design engineer may want to know the velocity distributions that can be expected for a given flow rate through an annulus. From a knowledge of the geometry of the annulus and the density of the fluid, he can calculate an average fluid velocity. By employing an approximate ratio of average to maximum velocity, say 0.9, an estimate of the maximum velocity can be obtained. If the viscosity of the fluid is known the model can be used to calculate the desired information. A check can then be made on the agreement between the calculated and desired mean velocity and if the desired accuracy is not obtained the estimated maximum velocity can be adjusted and the procedure repeated.

As the study is reviewed, it should be mentioned that the application of a diffusivity model to study turbulent flow in annuli yields the greatest benefits for annuli with small core-to-shell ratios. For annuli with core-to-shell ratios greater than about 0.6, the shear stress distributions are essentially linear and published universal velocity distribution laws can be employed. For smaller core-to-shell ratios, however, the universal velocity distribution laws fail to predict the marked distinction between the velocity distributions for the two flow regions. It is for these latter systems that the diffusivity model concept should provide a much needed tool for engineering applications.

CONCLUSIONS AND RECOMMENDATIONS

It has been shown that an eddy diffusivity model can be developed which will predict velocity distributions for turbulent flow in annuli within the scatter of experimental data. The effectiveness of the model depends upon the eddy diffusivity expressions employed and an expression relating maximum velocity radius to the core-to-shell ratio of an annulus. The study conducted here was undertaken to determine the applicability of diffusivity models and no attempt was made to examine the numerous diffusivity expressions available. It is recommended that future work be directed to studying more of these expressions, and perhaps extending the study to systems of other geometries.

LIST OF SYMBOLSEnglish Letter Symbols

a,b	Constants in equation 23
c,d	Constants in equation 24
f,g	Constants in equations 25a and 25b
h,j	Constants in equations 26a and 26b
K	Coefficient in equation 17
L	Length
n	Coefficient in equation 16
P	Pressure
r	Radius to a point in an annulus formed by two concentric cylinders
$r_c$	Outside radius of inner cylinder
$r_m$	Radius to point of maximum velocity
$r_s$	Inside radius of outer cylinder
u	Time-average axial velocity
$u^+$	Dimensionless (universal) velocity, $u/u^*$
$u^*$	Friction velocity at wall, $\sqrt{\tau_w/\rho}$
$u_m$	Maximum value of time-average axial velocity
$u_m^+$	Maximum value of universal velocity
y	Distance from cylinder wall
$y^+$	Dimensionless (universal) distance, $y\sqrt{\tau_w/\rho}/\nu$
$y_m^+$	Maximum value of universal distance

Greek Letter Symbols

$\alpha$	Ratio of radius of inner cylinder to radius of outer cylinder, $r_c/r_s$
$\epsilon$	Eddy diffusivity of momentum
$\nu$	Molecular diffusivity of momentum
$\mu$	Dynamic viscosity
$\gamma$	Kinematic viscosity, $\mu/\rho$
$\rho$	Mass density
$\tau$	Shear stress
$\tau_w$	Shear stress at the wall
$\tau_c$	Shear stress at wall of inner cylinder
$\tau_s$	Shear stress at wall of outer cylinder

Note: o Used as a subscript designates the outer region of flow in an annulus, i.e., the region bounded by the shell and the maximum velocity radius.

i Used as a subscript designates the inner region of flow in an annulus, i.e., the region bounded by the maximum velocity radius and the core.

# FIGURE 1

VARIATION OF MAXIMUM VELOCITY RADIUS  
WITH CORE-TO-SHELL RATIO OF AN ANNULUS

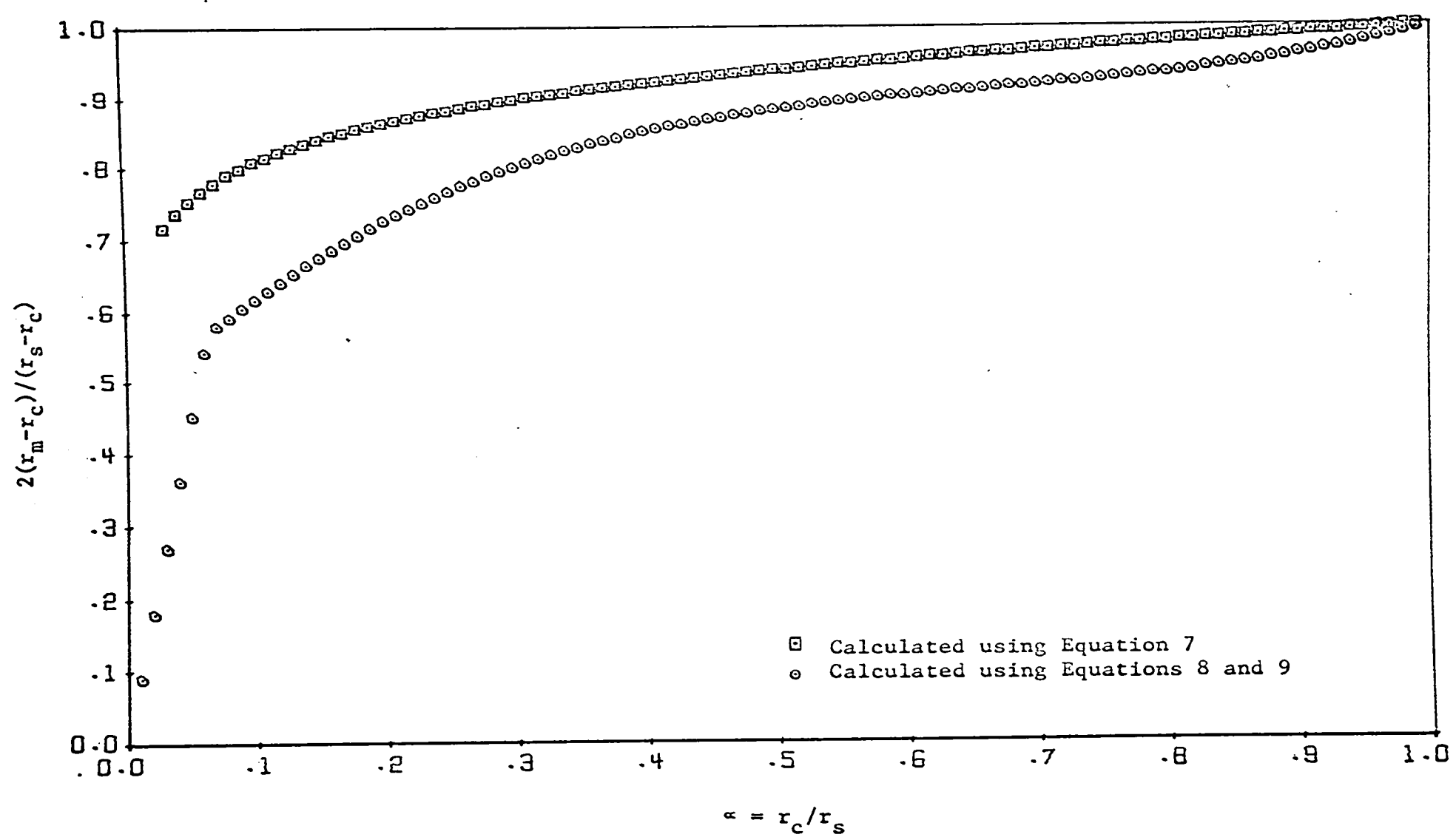


# FIGURE 2

NORMALIZED SHEAR STRESS DISTRIBUTIONS  
FOR ANNULI WITH DIFFERENT CORE-TO-SHELL RATIOS

Note: Eqn. 7 was used to locate the  
maximum velocity radius

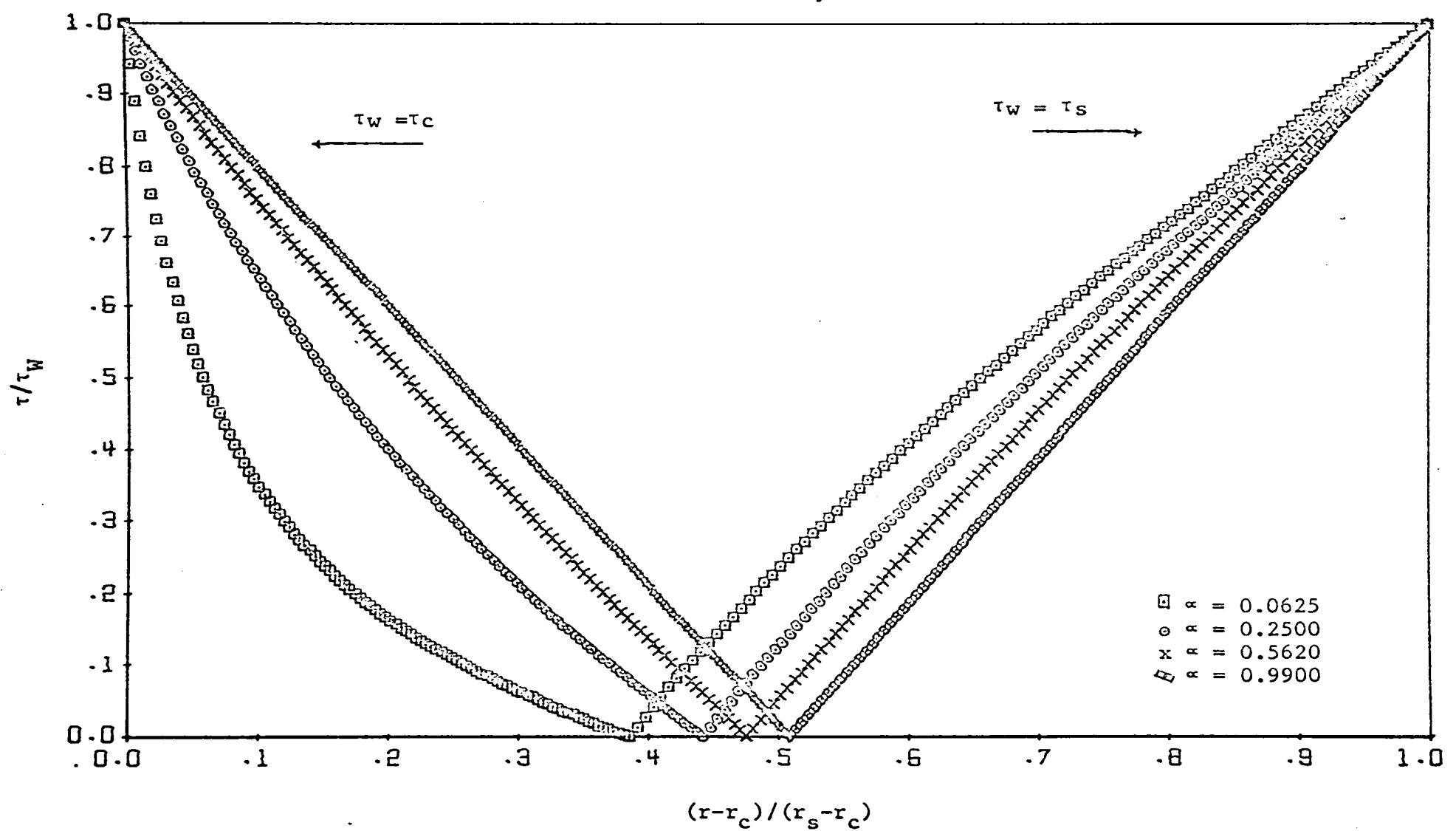


# FIGURE 3

NORMALIZED SHEAR STRESS DISTRIBUTIONS  
FOR ANNULI WITH DIFFERENT CORE-TO-SHELL RATIOS

Note: Eqn. 8 was used to locate the  
maximum velocity radius

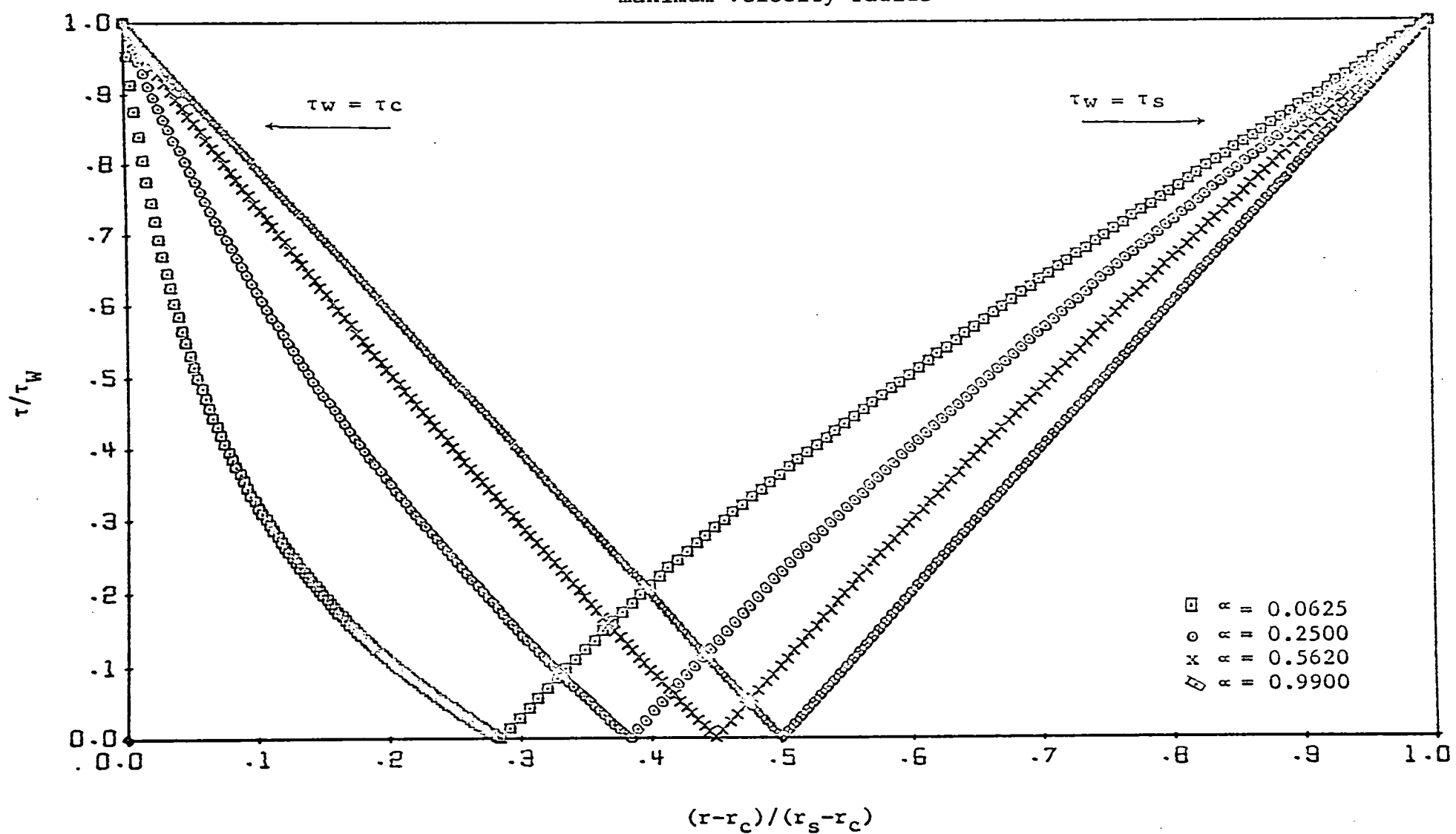




# FIGURE 4

UNIVERSAL VELOCITY DISTRIBUTIONS FOR AIR FLOWING IN AN ANNULUS  
WITH A CORE-TO-SHELL RATIO OF 0.0625 AT A MAXIMUM VELOCITY OF 30 FPS

Note: Eqn. 7 was used to locate the maximum velocity radius

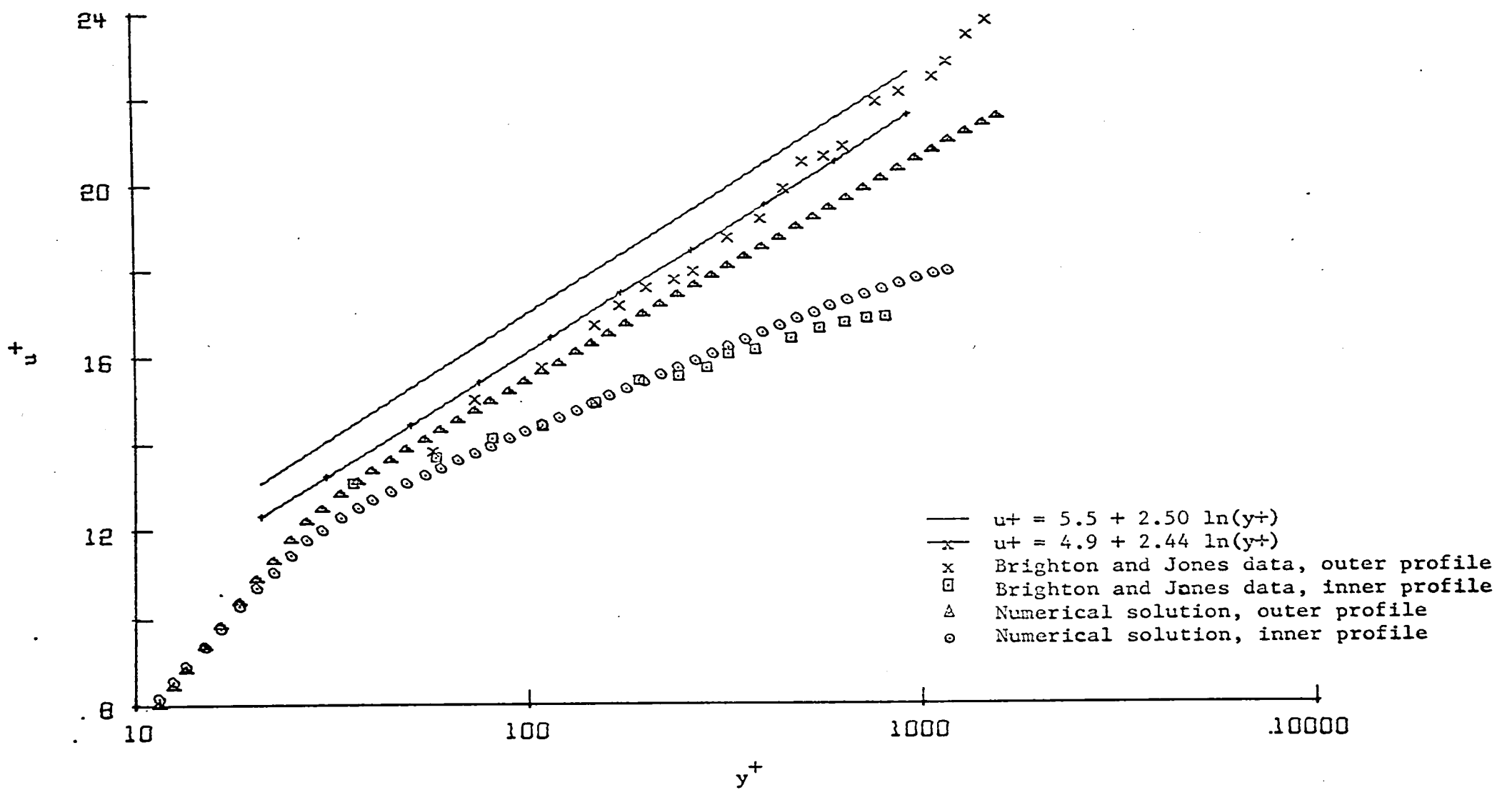


# FIGURE 5

UNIVERSAL VELOCITY DISTRIBUTIONS FOR AIR FLOWING IN AN ANNULUS  
WITH A CORE-TO-SHELL RATIO OF 0.0625 AT A MAXIMUM VELOCITY OF 60 FPS

Note: Eqn. 7 was used to locate the maximum velocity radius

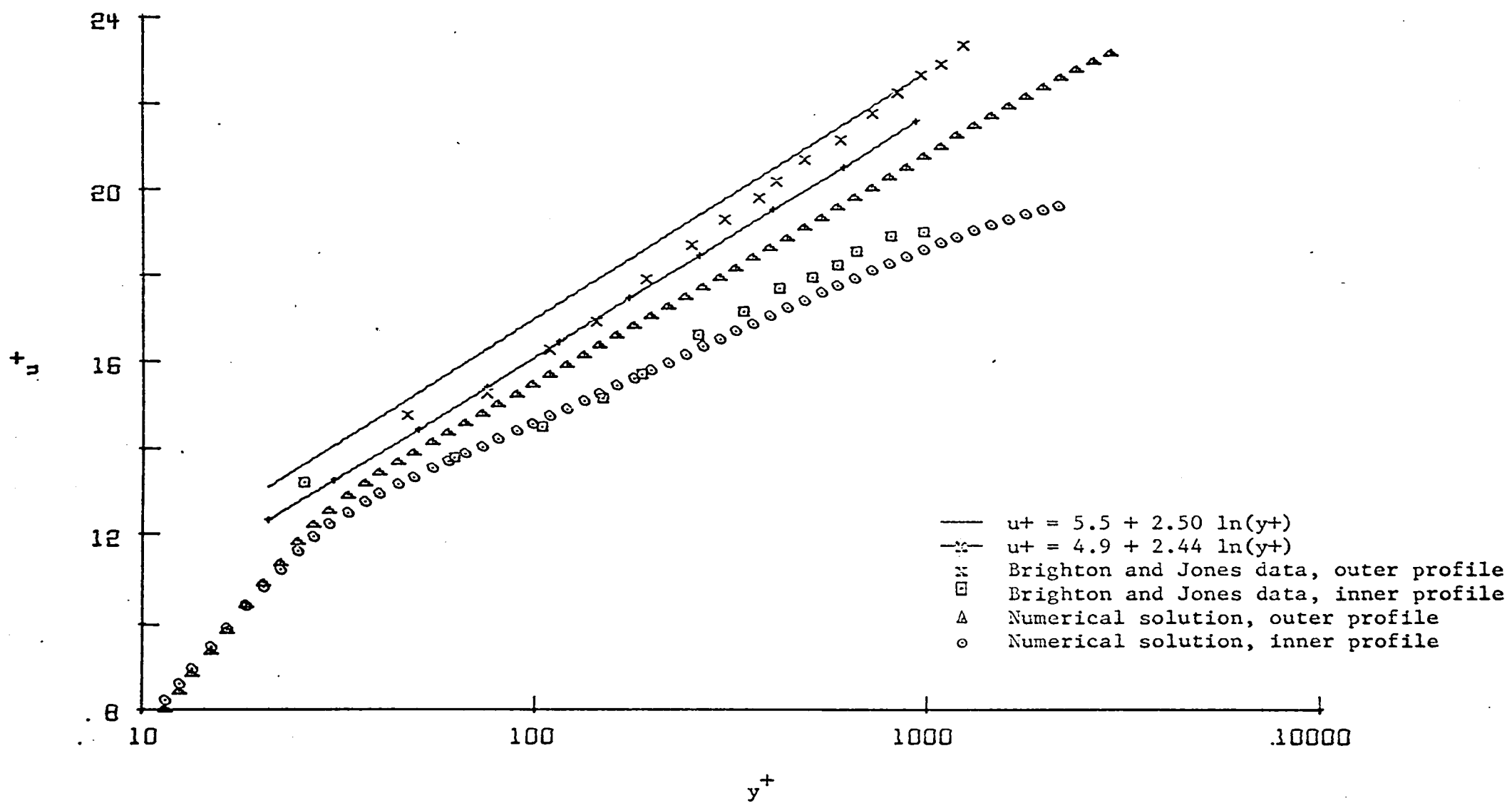


# FIGURE 6

UNIVERSAL VELOCITY DISTRIBUTIONS FOR AIR FLOWING IN AN ANNULUS  
WITH A CORE-TO-SHELL RATIO OF 0.5620 AT A MAXIMUM VELOCITY OF 30 FPS

Note: Eqn. 7 was used to locate the maximum velocity radius

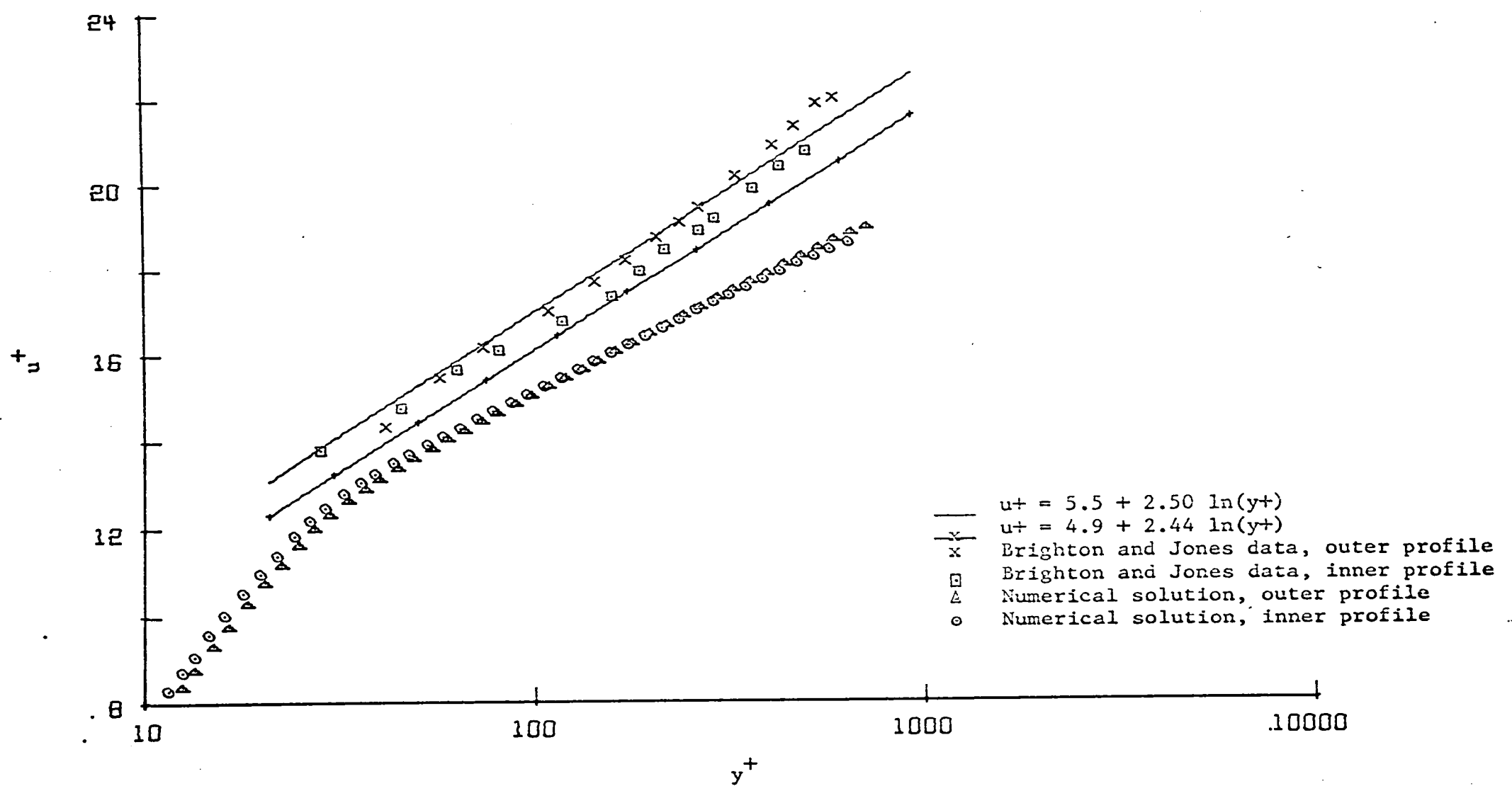


# FIGURE 7

UNIVERSAL VELOCITY DISTRIBUTIONS FOR AIR FLOWING IN AN ANNULUS  
WITH A CORE-TO-SHELL RATIO OF 0.5620 AT A MAXIMUM VELOCITY OF 60 FPS

Note: Eqn. 7 was used to locate the maximum velocity radius

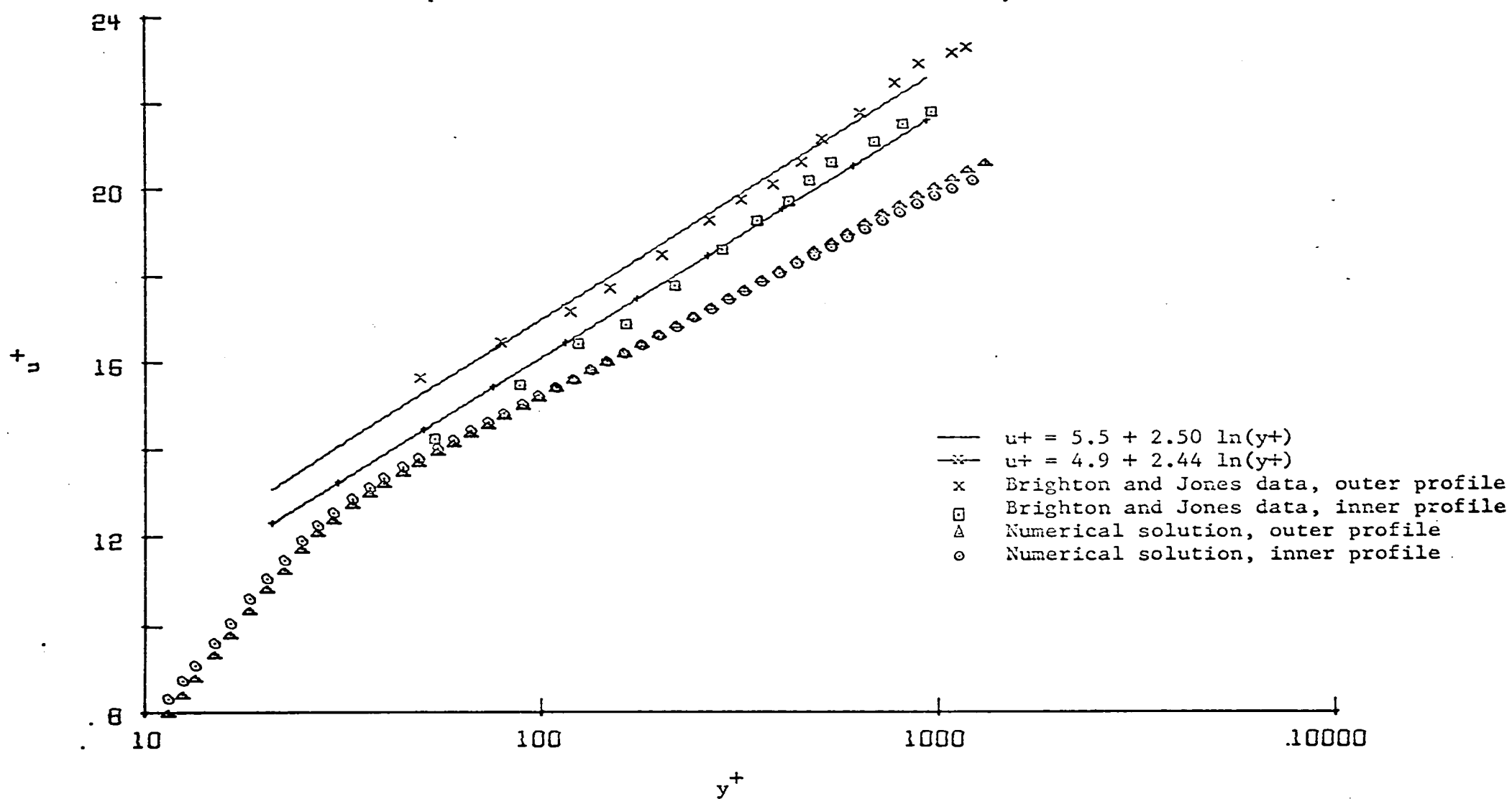


# FIGURE 8

MEAN VELOCITY PROFILES FOR AIR FLOWING IN AN ANNULUS  
WITH A CORE-TO-SHELL RATIO OF 0.0625 AT A MAXIMUM VELOCITY OF 30 FPS

Note: Eqn. 7 was used to locate the maximum velocity radius

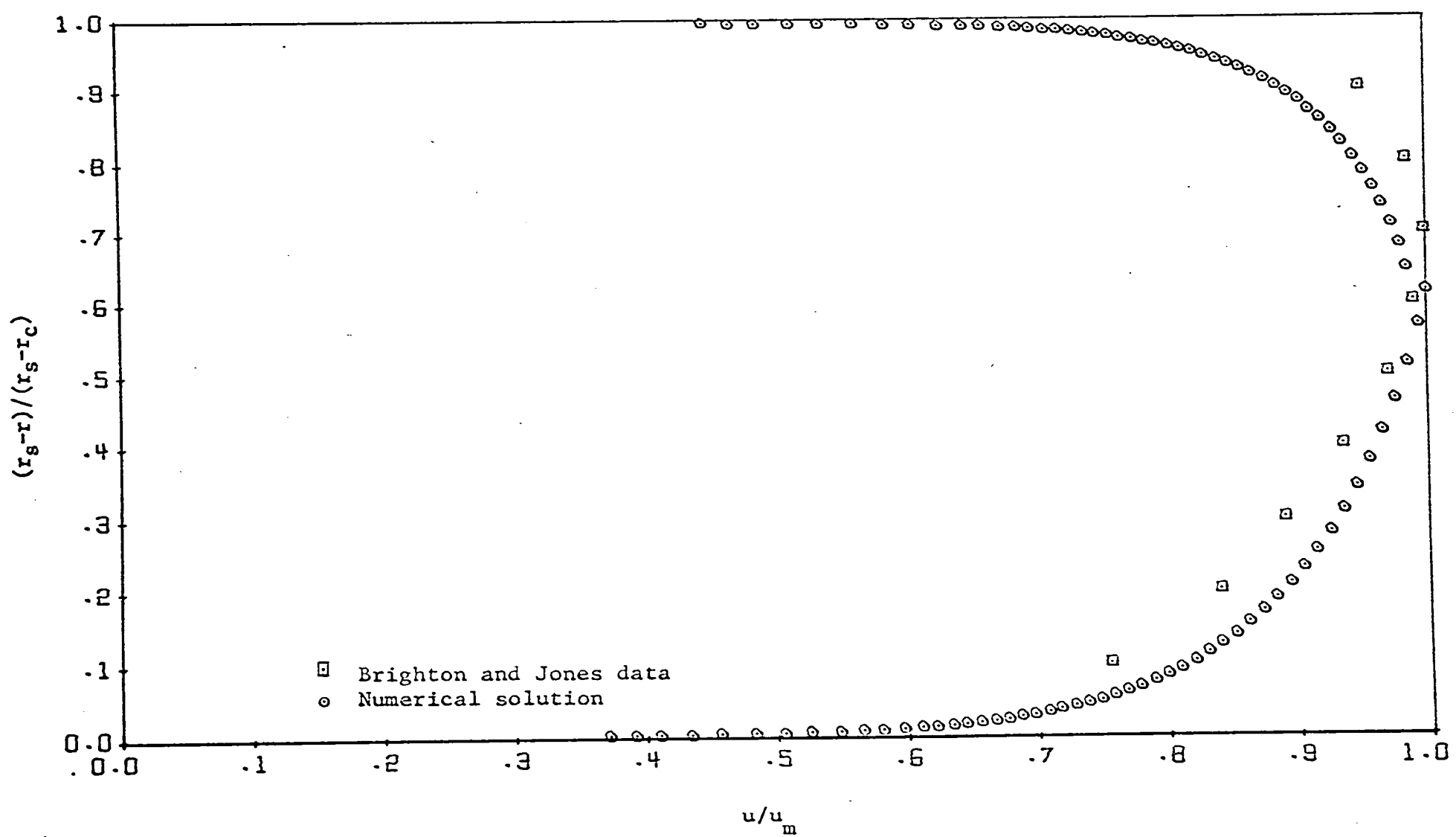


# FIGURE 9

MEAN VELOCITY PROFILES FOR AIR FLOWING IN AN ANNULUS  
WITH A CORE-TO-SHELL RATIO OF 0.0625 AT A MAXIMUM VELOCITY OF 60 FPS

Note: Eqn. 7 was used to locate the maximum velocity radius

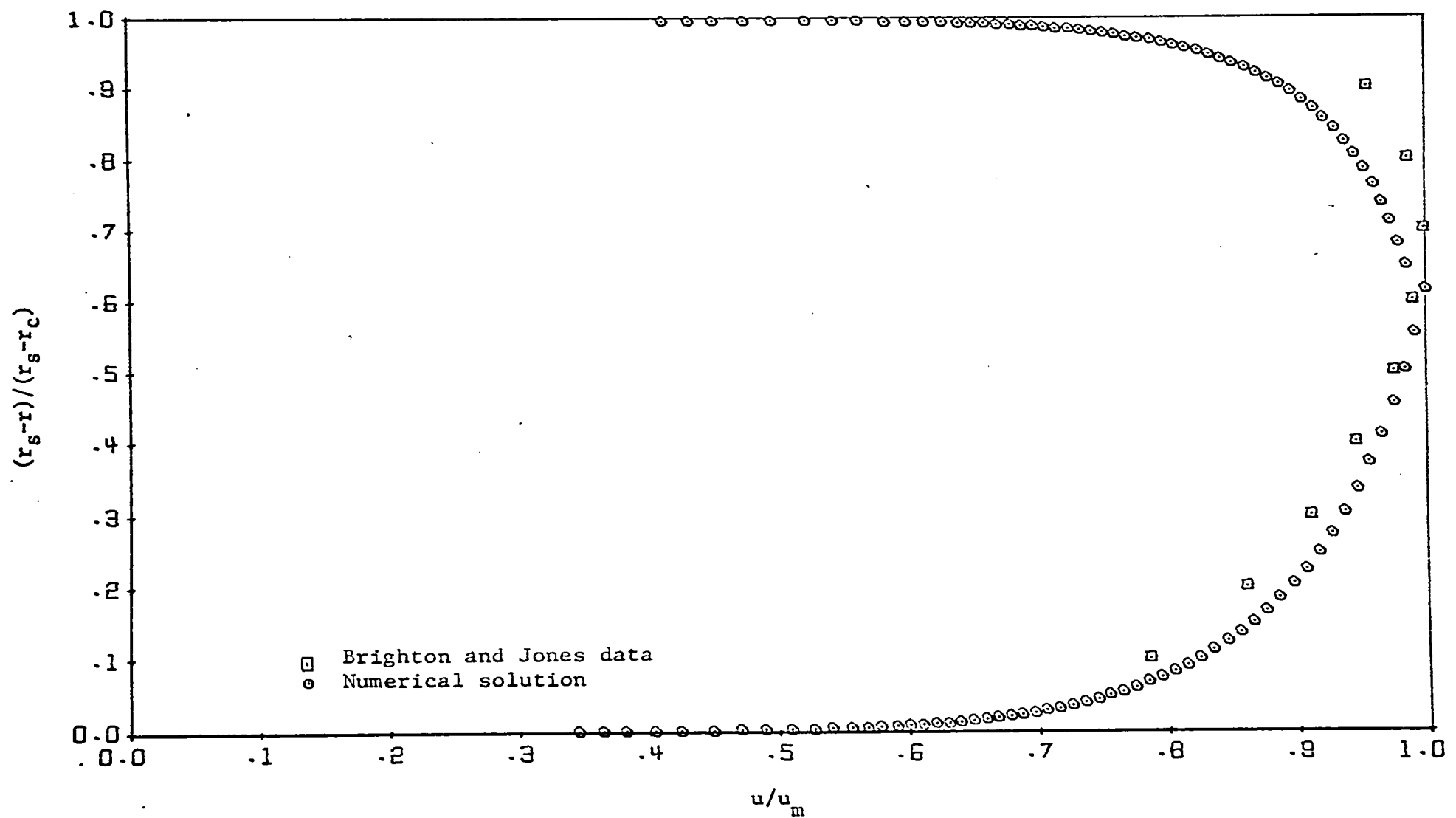
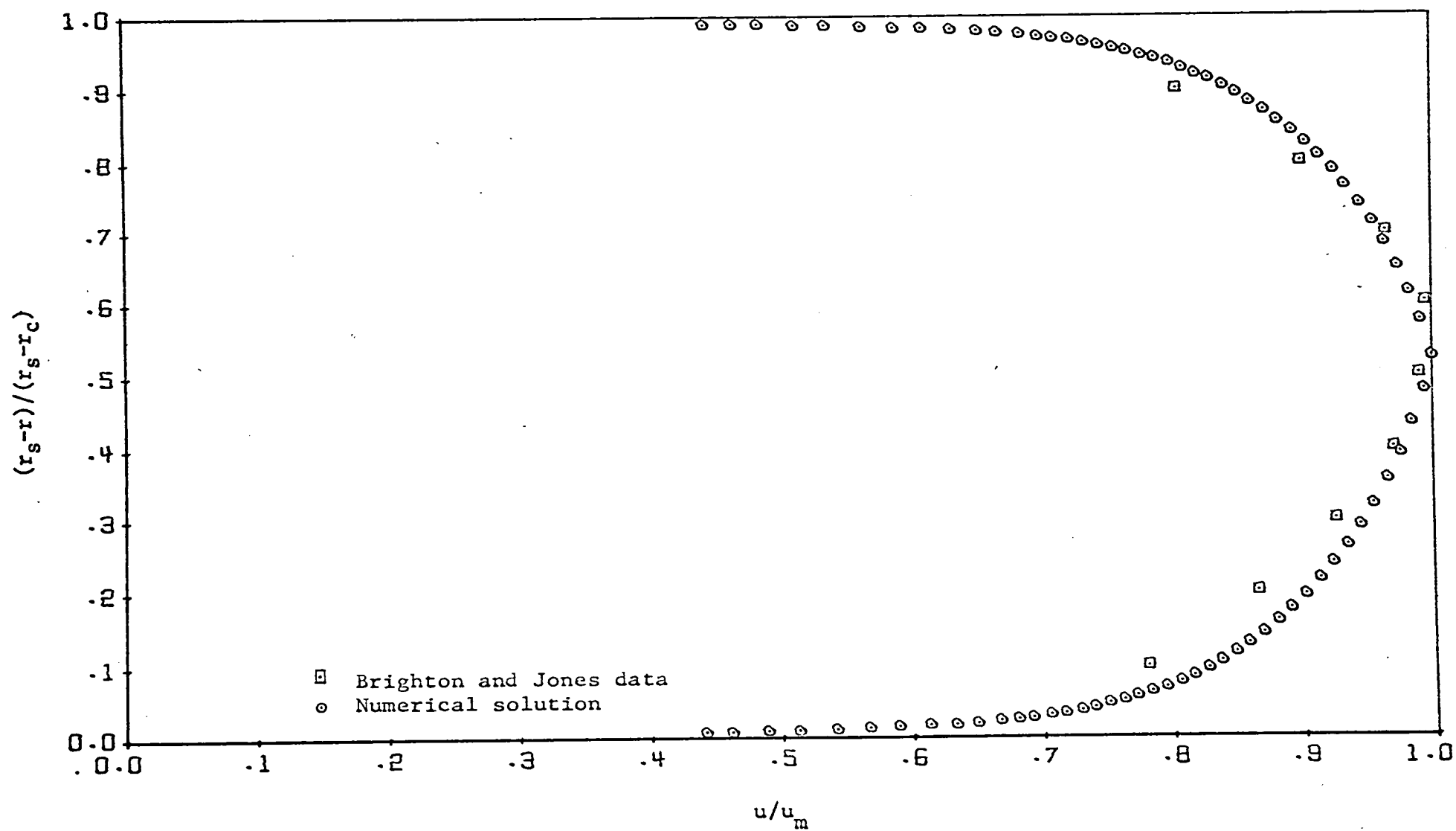


FIGURE 10

MEAN VELOCITY PROFILES FOR AIR FLOWING IN AN ANNULUS  
WITH A CORE-TO-SHELL RATIO OF 0.5620 AT A MAXIMUM VELOCITY OF 30 FPS

Note: Eqn. 7 was used to locate the maximum velocity radius



# FIGURE 11

MEAN VELOCITY PROFILES FOR AIR FLOWING IN AN ANNULUS  
WITH A CORE-TO-SHELL RATIO OF 0.5620 AT A MAXIMUM VELOCITY OF 60 FPS

Note: Eqn. 7 was used to locate the maximum velocity radius

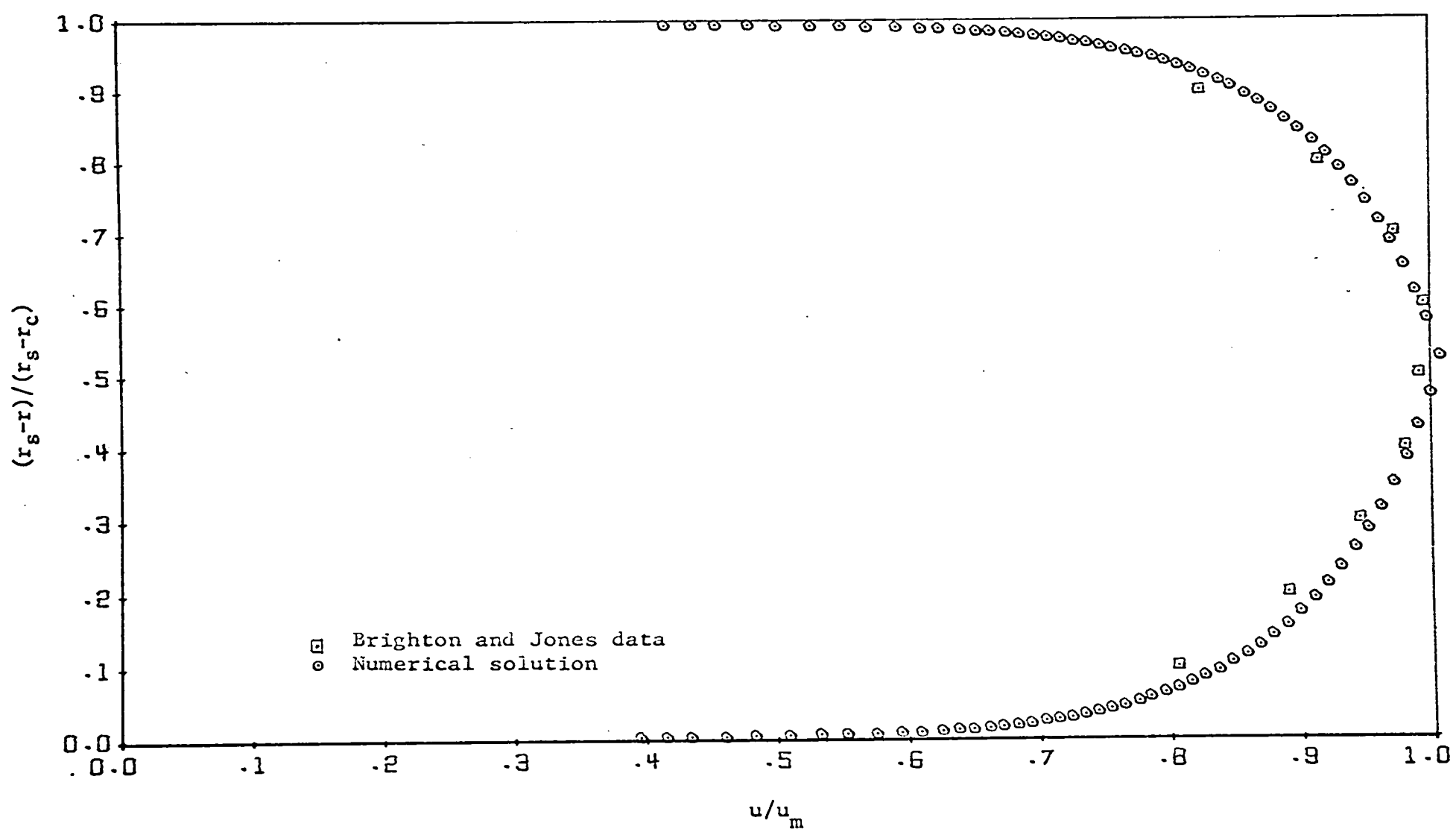




# FIGURE 12

UNIVERSAL VELOCITY DISTRIBUTIONS FOR AIR FLOWING IN AN ANNULUS  
WITH A CORE-TO-SHELL RATIO OF 0.0625 AT A MAXIMUM VELOCITY OF 30 FPS

Note: Eqn. 8 was used to locate the maximum velocity radius

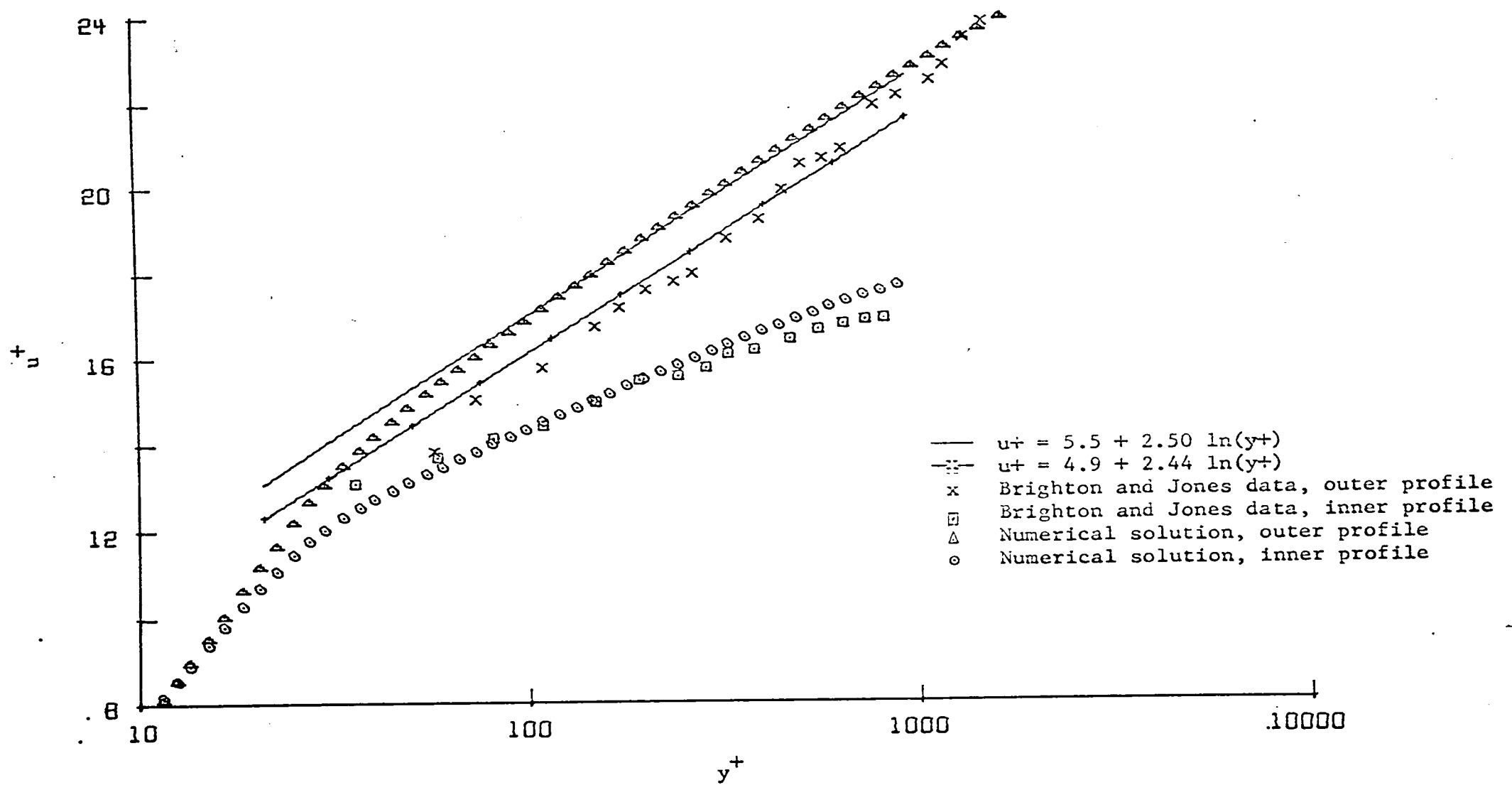


# FIGURE 13

UNIVERSAL VELOCITY DISTRIBUTIONS FOR AIR FLOWING IN AN ANNULUS  
WITH A CORE-TO-SHELL RATIO OF 0.0625 AT A MAXIMUM VELOCITY OF 60 FPS

Note: Eqn. 8 was used to locate the maximum velocity radius

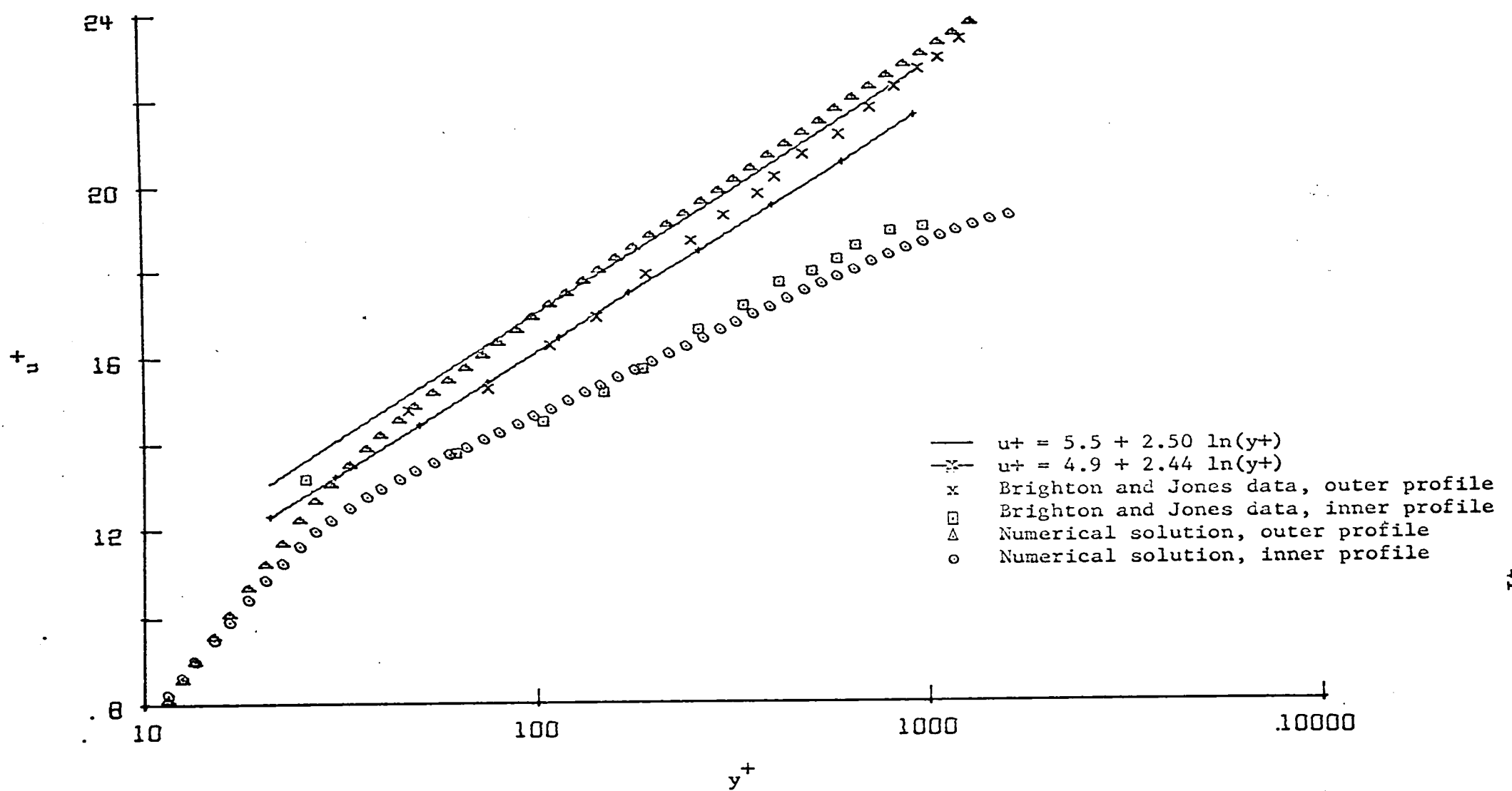


# FIGURE 14

UNIVERSAL VELOCITY DISTRIBUTIONS FOR AIR FLOWING IN AN ANNULUS  
WITH A CORE-TO-SHELL RATIO OF 0.5620 AT A MAXIMUM VELOCITY OF 30 FPS

Note: Eqn. 8 was used to locate the maximum velocity radius

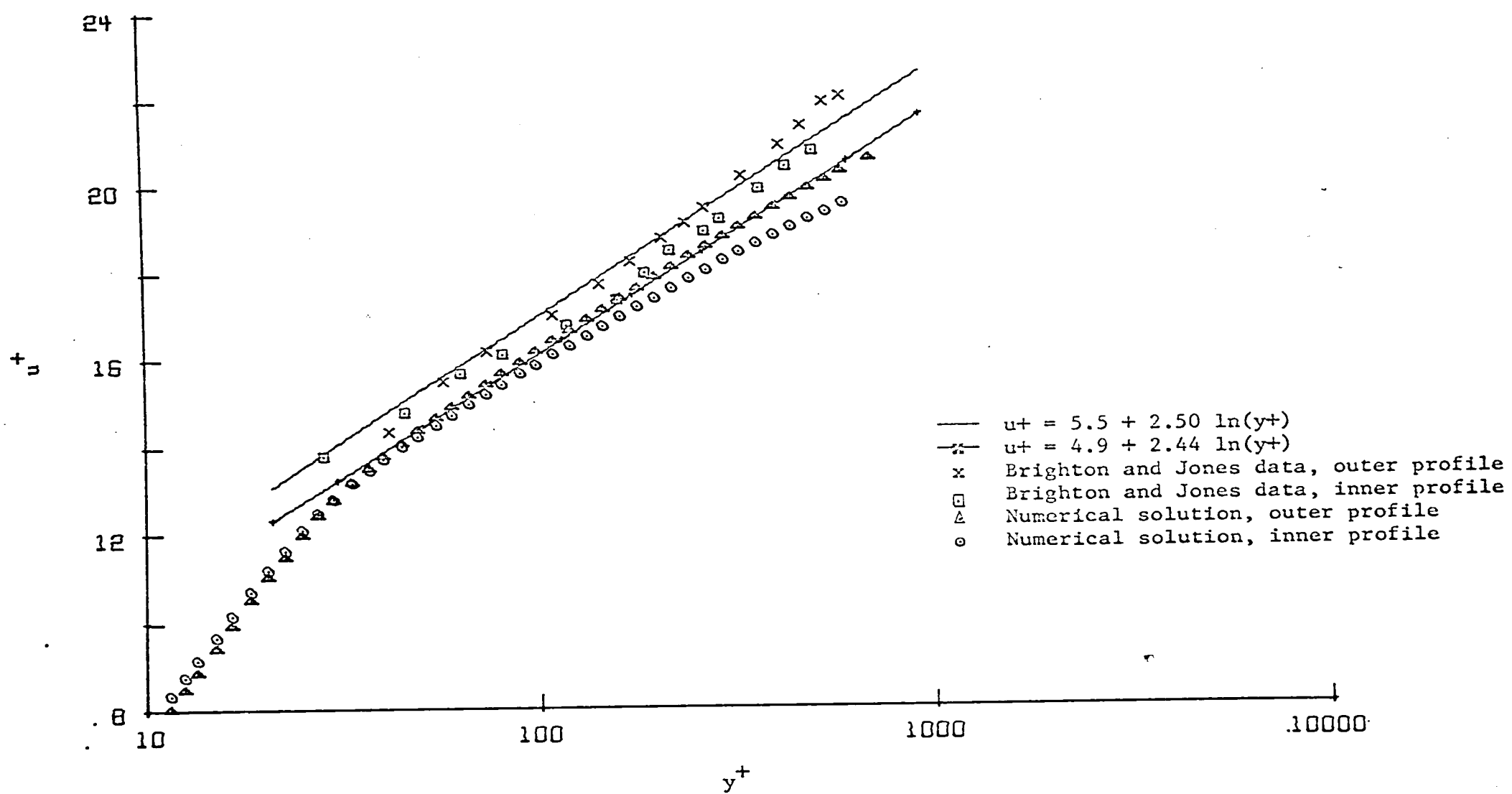


# FIGURE 15

UNIVERSAL VELOCITY DISTRIBUTIONS FOR AIR FLOWING IN AN ANNULUS  
WITH A CORE-TO-SHELL RATIO OF 0.5620 AT A MAXIMUM VELOCITY OF 60 FPS

Note: Eqn. 8 was used to locate the maximum velocity radius

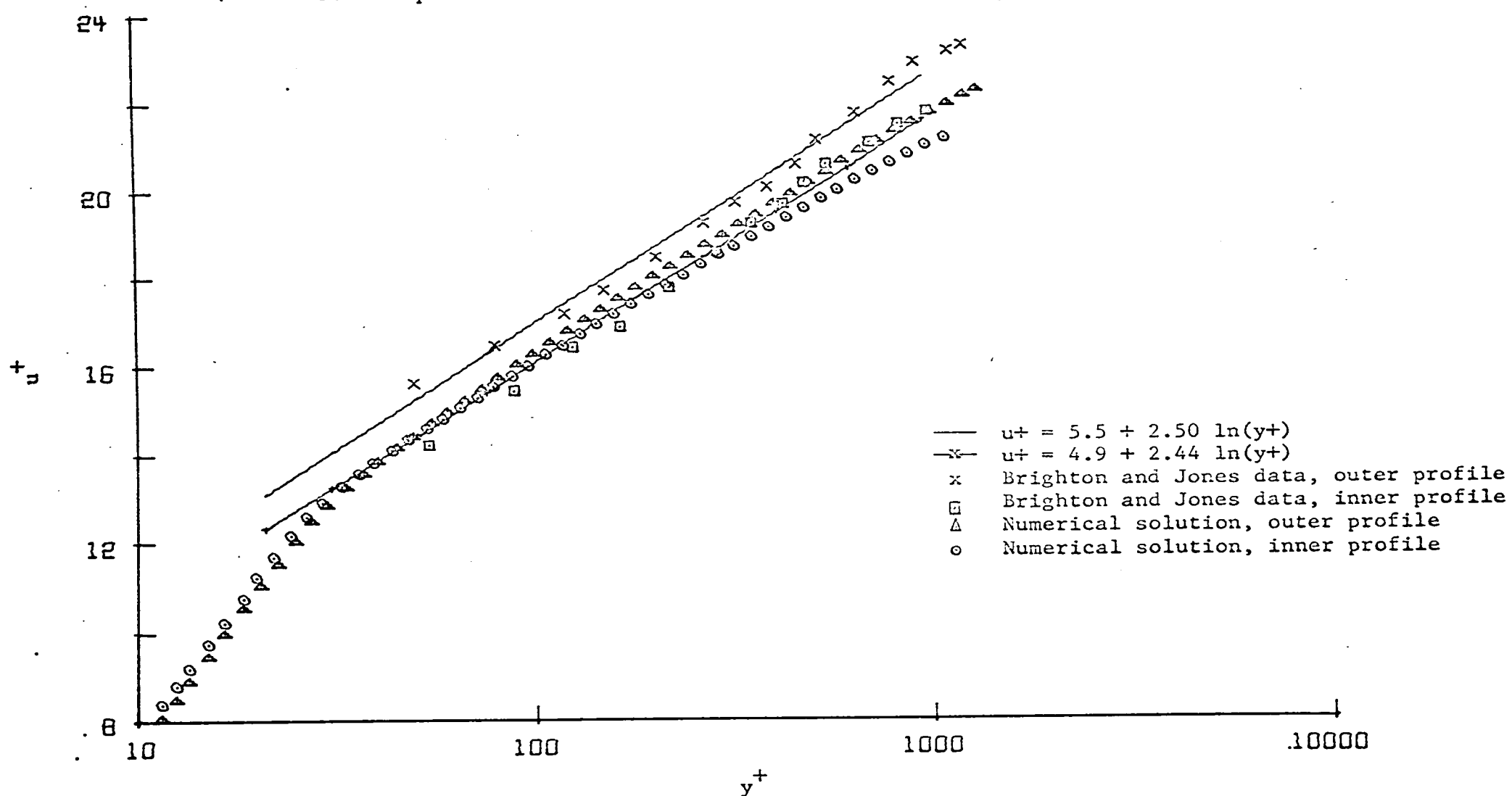


# FIGURE 16

MEAN VELOCITY PROFILES FOR AIR FLOWING IN AN ANNULUS  
WITH A CORE-TO-SHELL RATIO OF 0.0625 AT A MAXIMUM VELOCITY OF 30 FPS

Note: Eqn. 8 was used to locate the maximum velocity radius

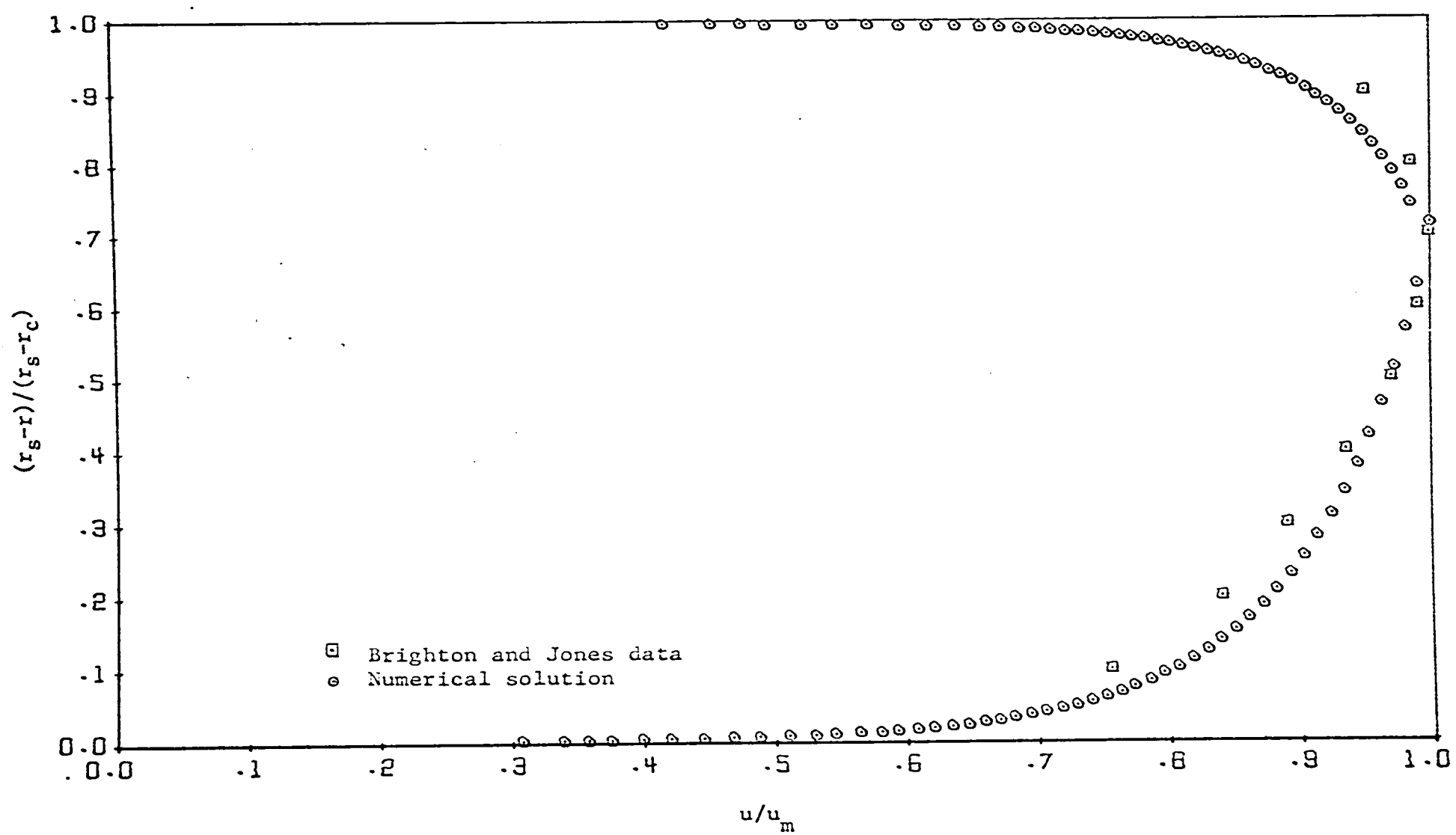


# FIGURE 17

MEAN VELOCITY PROFILES FOR AIR FLOWING IN AN ANNULUS  
WITH A CORE-TO-SHELL RATIO OF 0.0625 AT A MAXIMUM VELOCITY OF 60 FPS

Note: Eqn. 8 was used to locate the maximum velocity radius

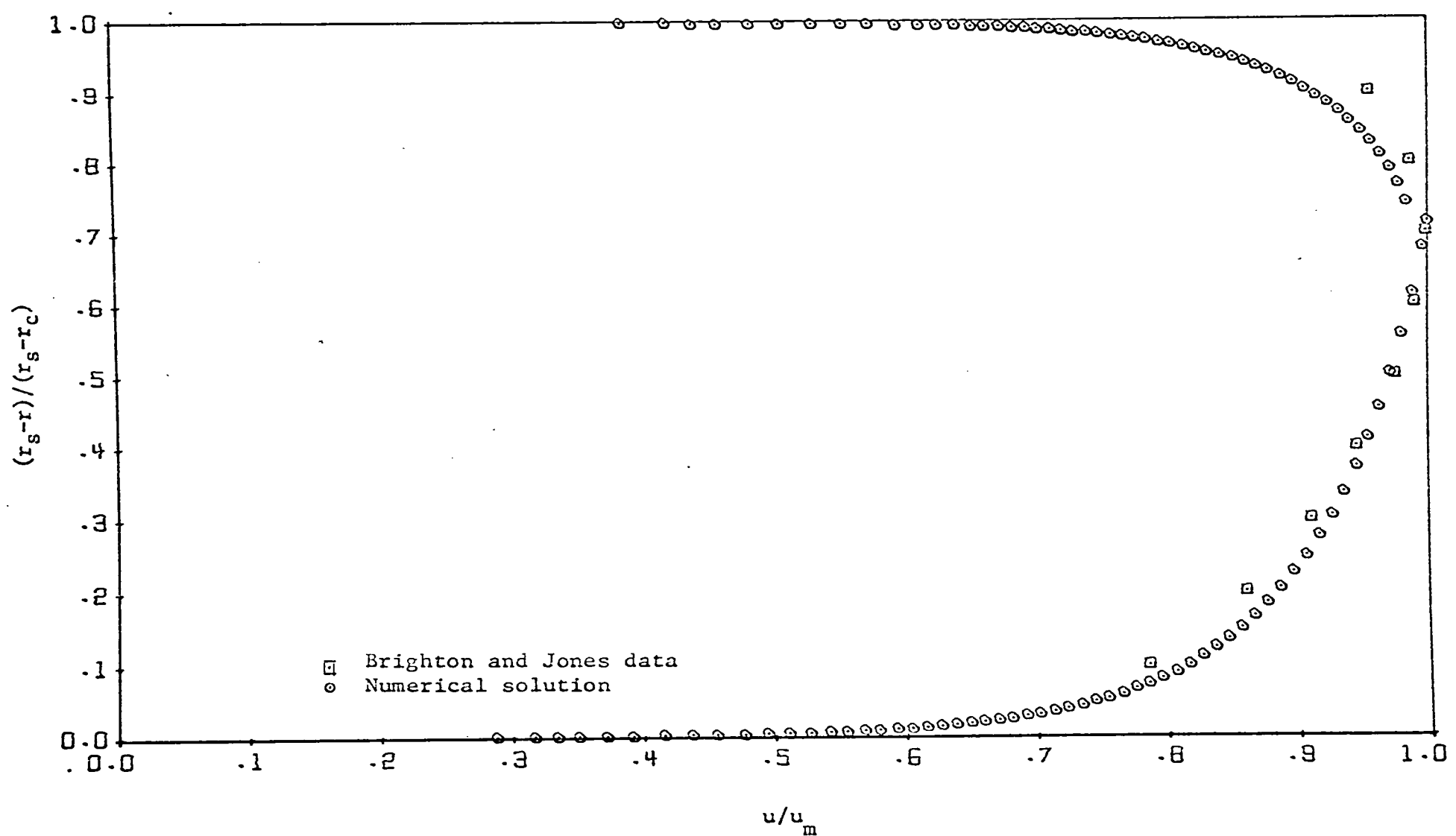


# FIGURE 18

MEAN VELOCITY PROFILES FOR AIR FLOWING IN AN ANNULUS  
WITH A CORE-TO-SHELL RATIO OF 0.5620 AT A MAXIMUM VELOCITY OF 30 FPS

Note: Eqn. 8 was used to locate the maximum velocity radius

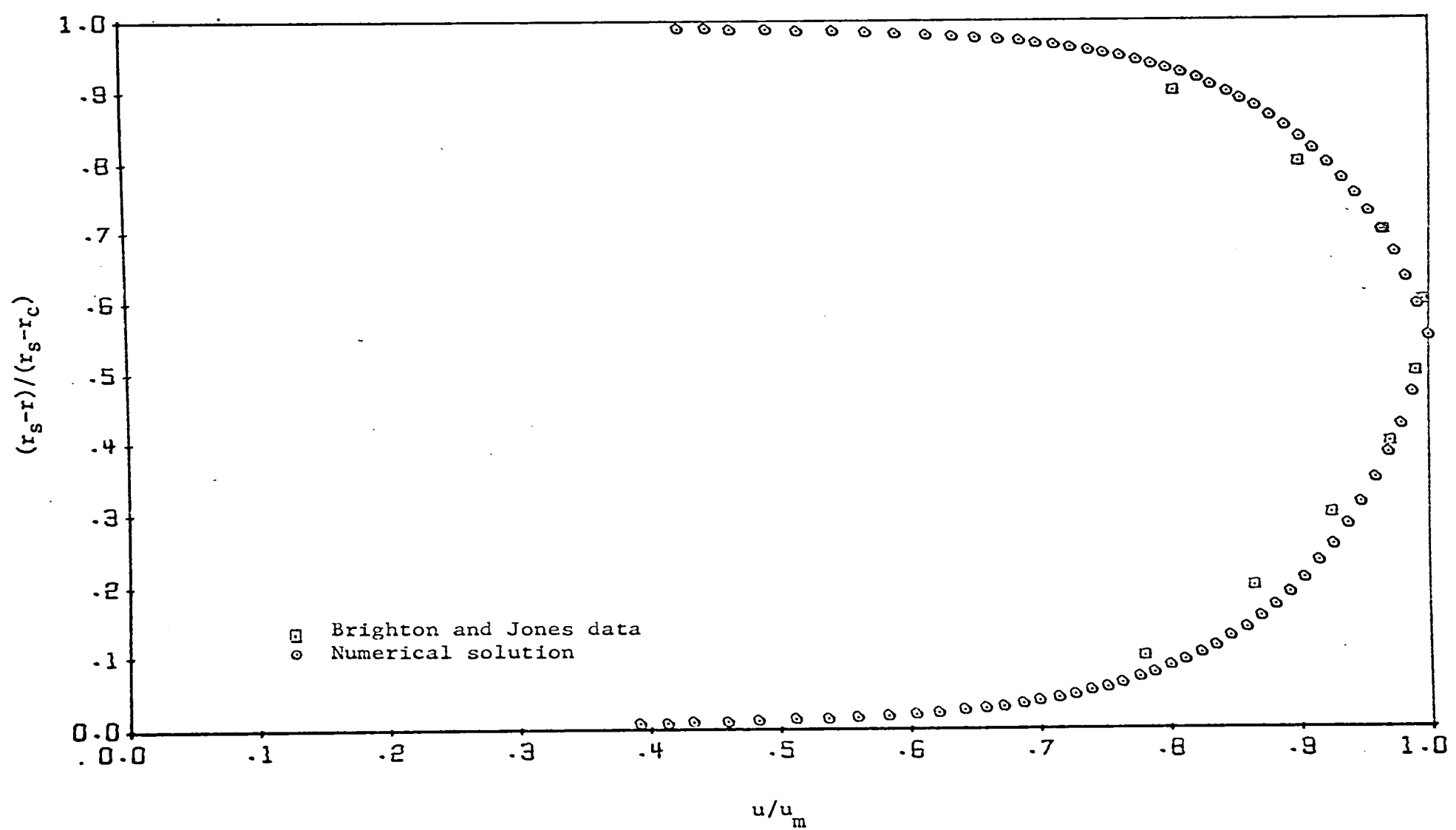


# FIGURE 19

MEAN VELOCITY PROFILES FOR AIR FLOWING IN AN ANNULUS  
WITH A CORE-TO-SHELL RATIO OF 0.5620 AT A MAXIMUM VELOCITY OF 60 FPS

Note: Eqn. 8 was used to locate the maximum velocity radius

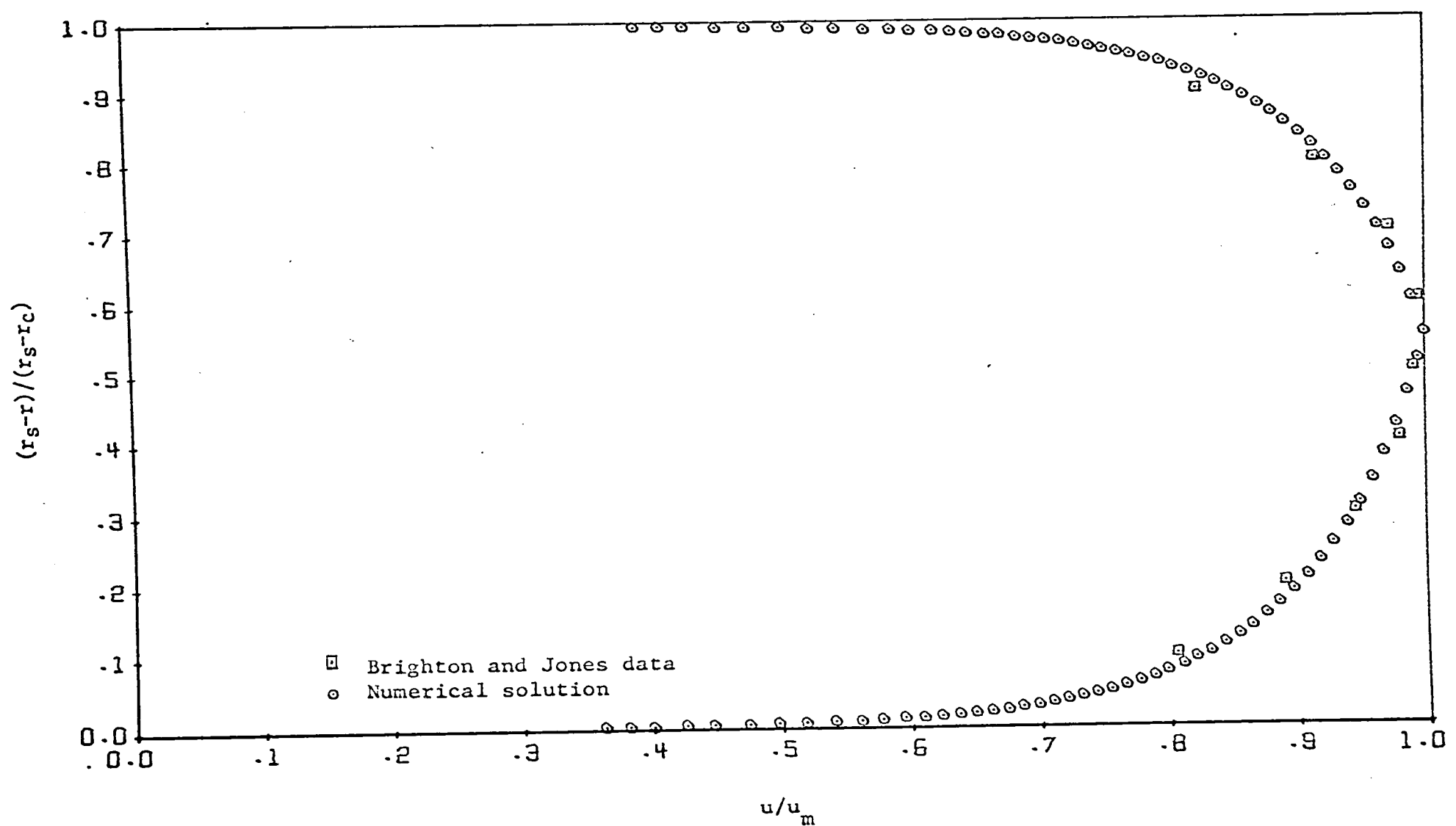




# FIGURE 20

UNIVERSAL VELOCITY DISTRIBUTIONS FOR AIR FLOWING IN AN ANNULUS  
WITH A CORE-TO-SHELL RATIO OF 0.0010 AT A MAXIMUM VELOCITY OF 30 FPS

Note: Eqn. 8 was used to locate the maximum velocity radius

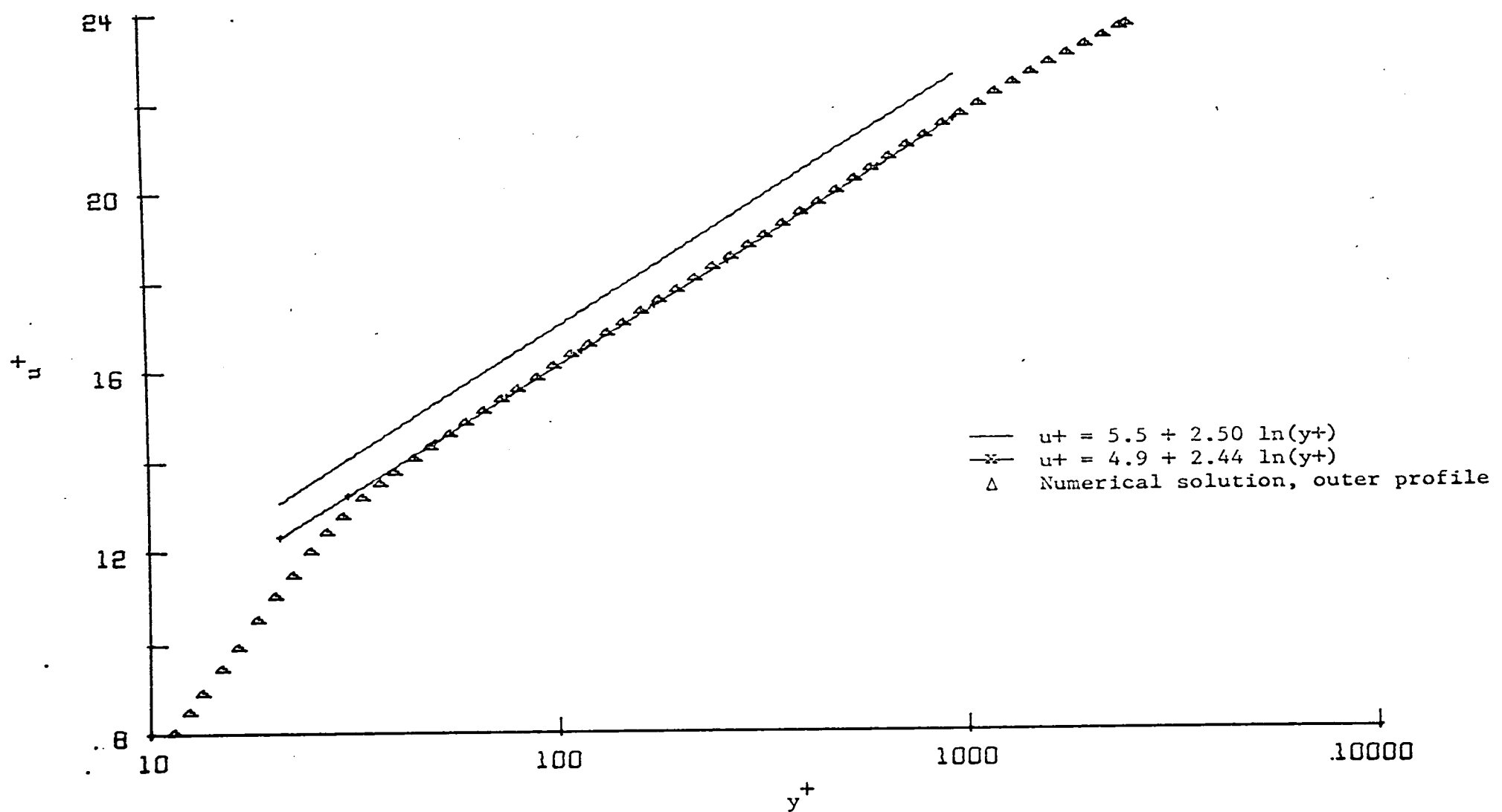


# FIGURE 21

UNIVERSAL VELOCITY DISTRIBUTIONS FOR AIR FLOWING IN AN ANNULUS  
WITH A CORE-TO-SHELL RATIO OF 0.0010 AT A MAXIMUM VELOCITY OF 60 FPS

Note: Eqn. 8 was used to locate the maximum velocity radius

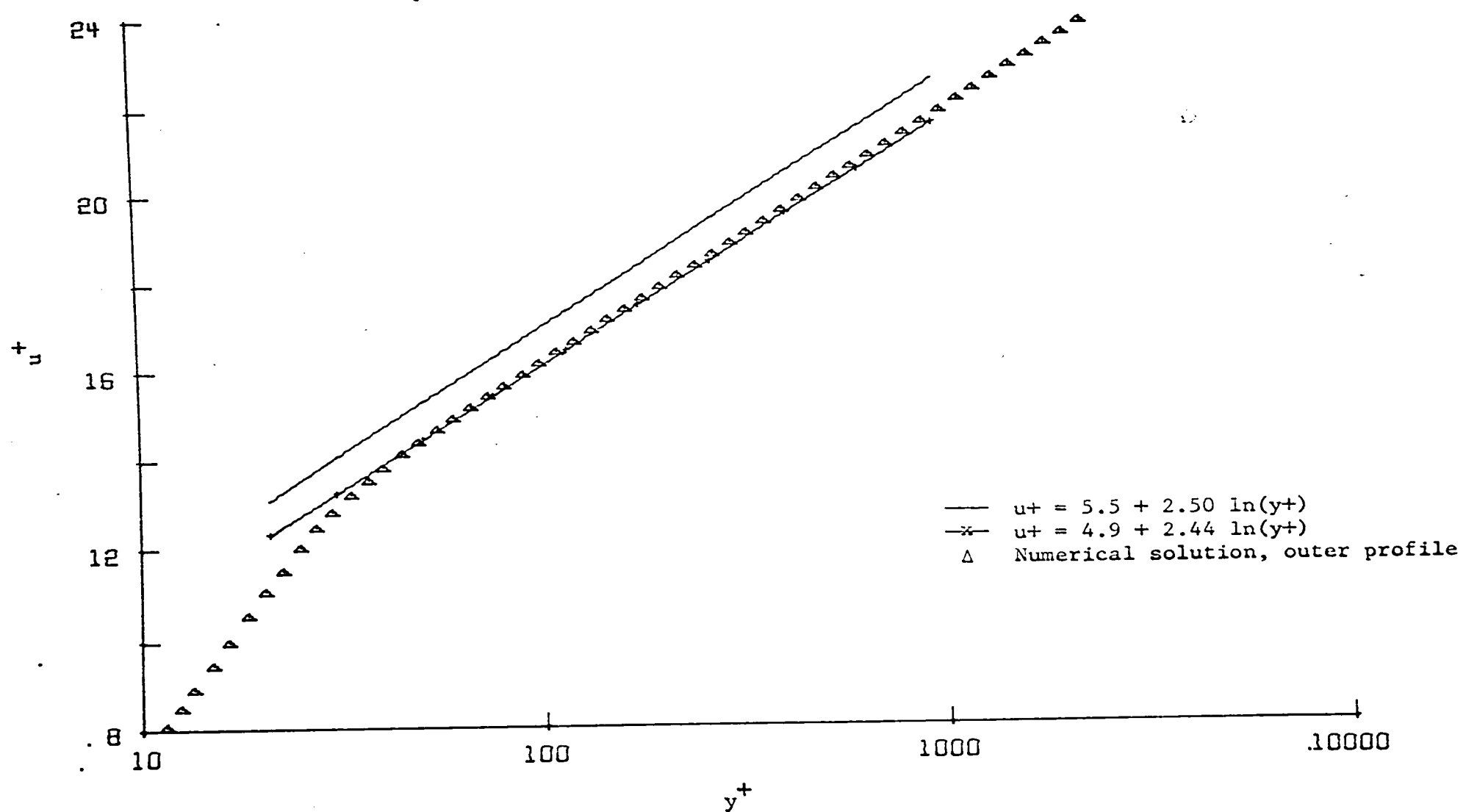


# FIGURE 22

UNIVERSAL VELOCITY DISTRIBUTIONS FOR AIR FLOWING IN AN ANNULUS  
WITH A CORE-TO-SHELL RATIO OF 0.9900 AT A MAXIMUM VELOCITY OF 30 FPS

Note: Eqn. 8 was used to locate the maximum velocity radius

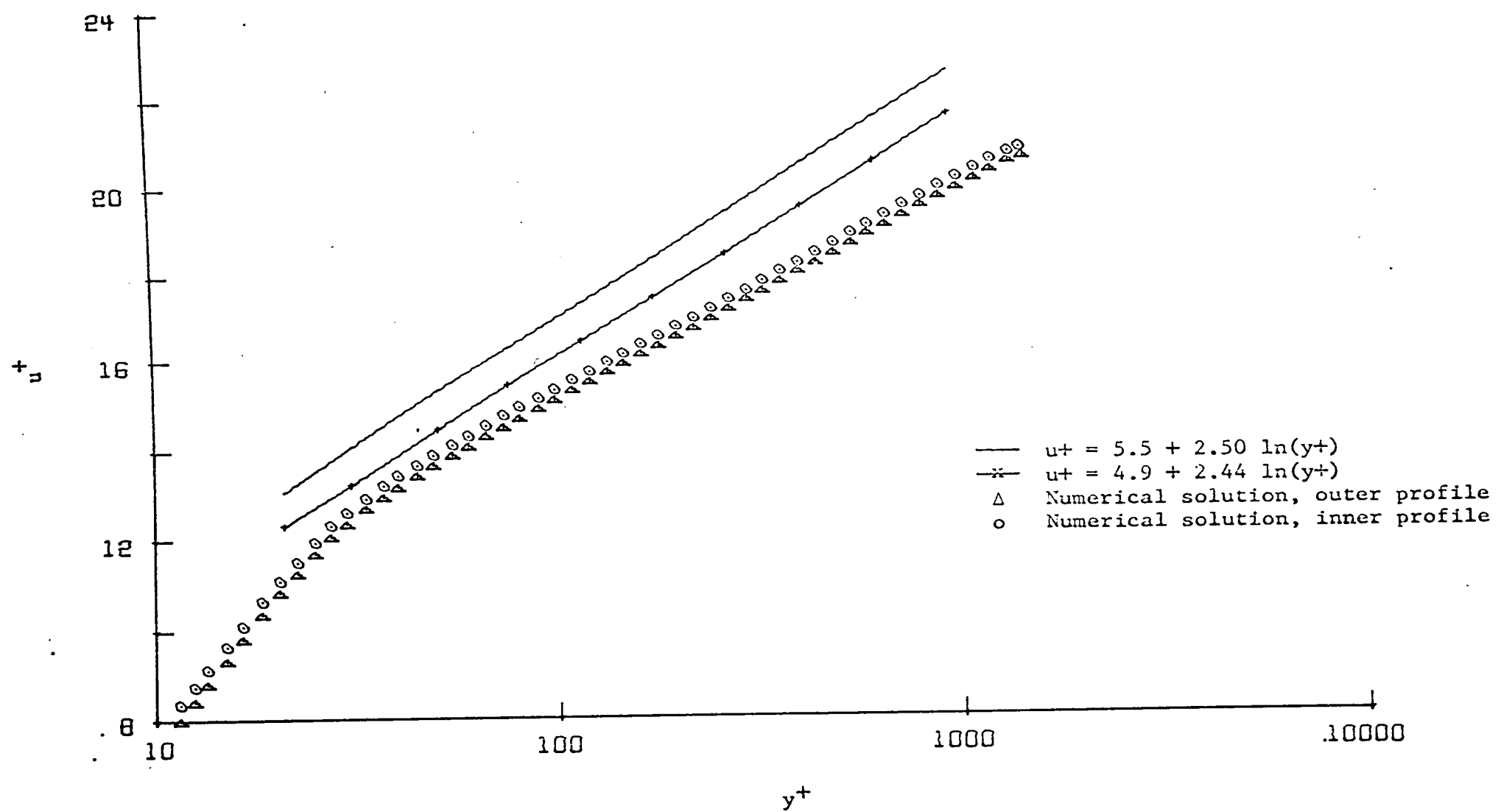


# FIGURE 23

UNIVERSAL VELOCITY DISTRIBUTIONS FOR AIR FLOWING IN AN ANNULUS  
WITH A CORE-TO-SHELL RATIO OF 0.9900 AT A MAXIMUM VELOCITY OF 60 FPS

Note: Eqn. 8 was used to locate the maximum velocity radius

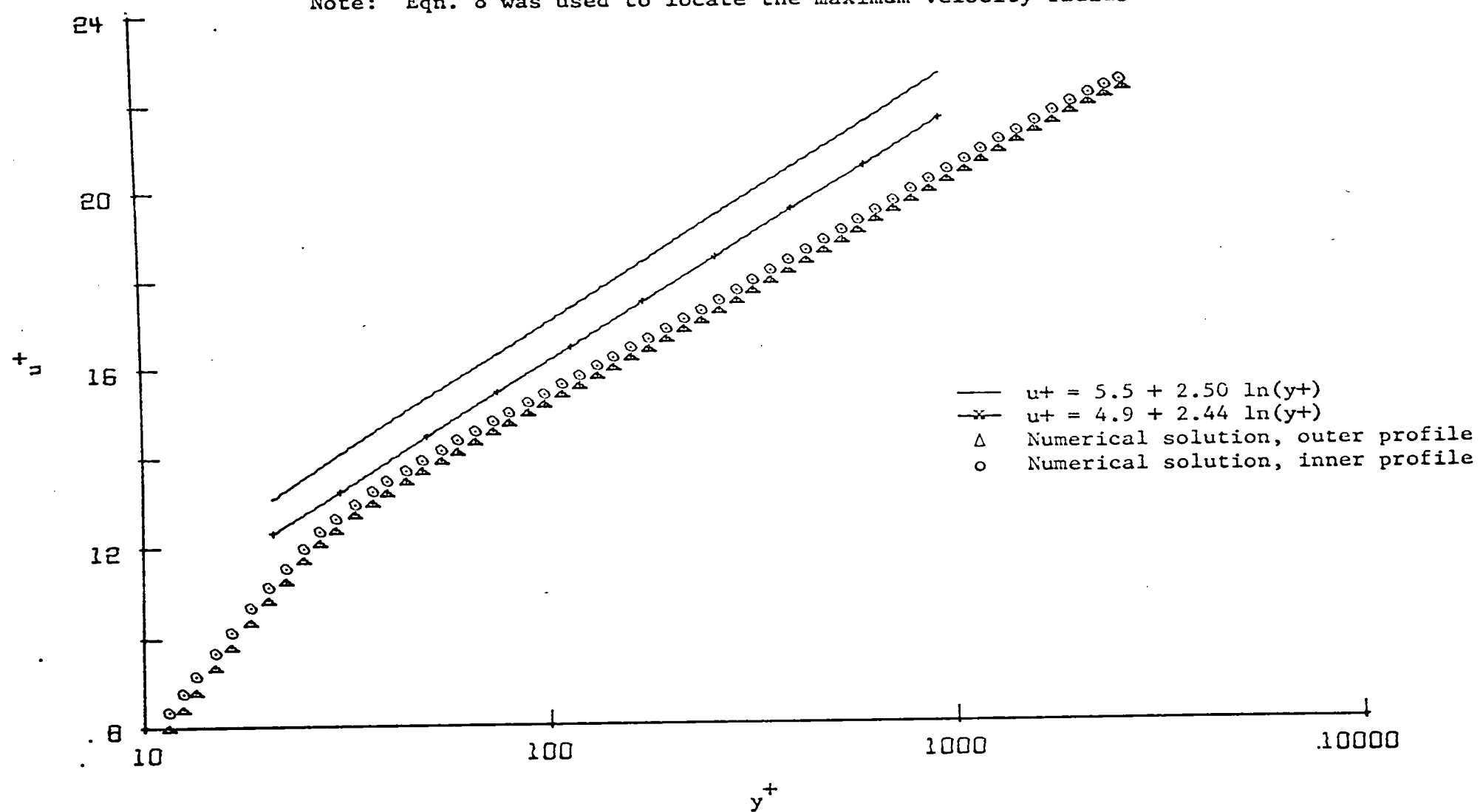


# FIGURE 24

MEAN VELOCITY PROFILE FOR AIR FLOWING IN AN ANNULUS  
WITH A CORE-TO-SHELL RATIO OF 0.0010 AT A MAXIMUM VELOCITY OF 30 FPS

Note: Eqn. 8 was used to locate the maximum velocity radius

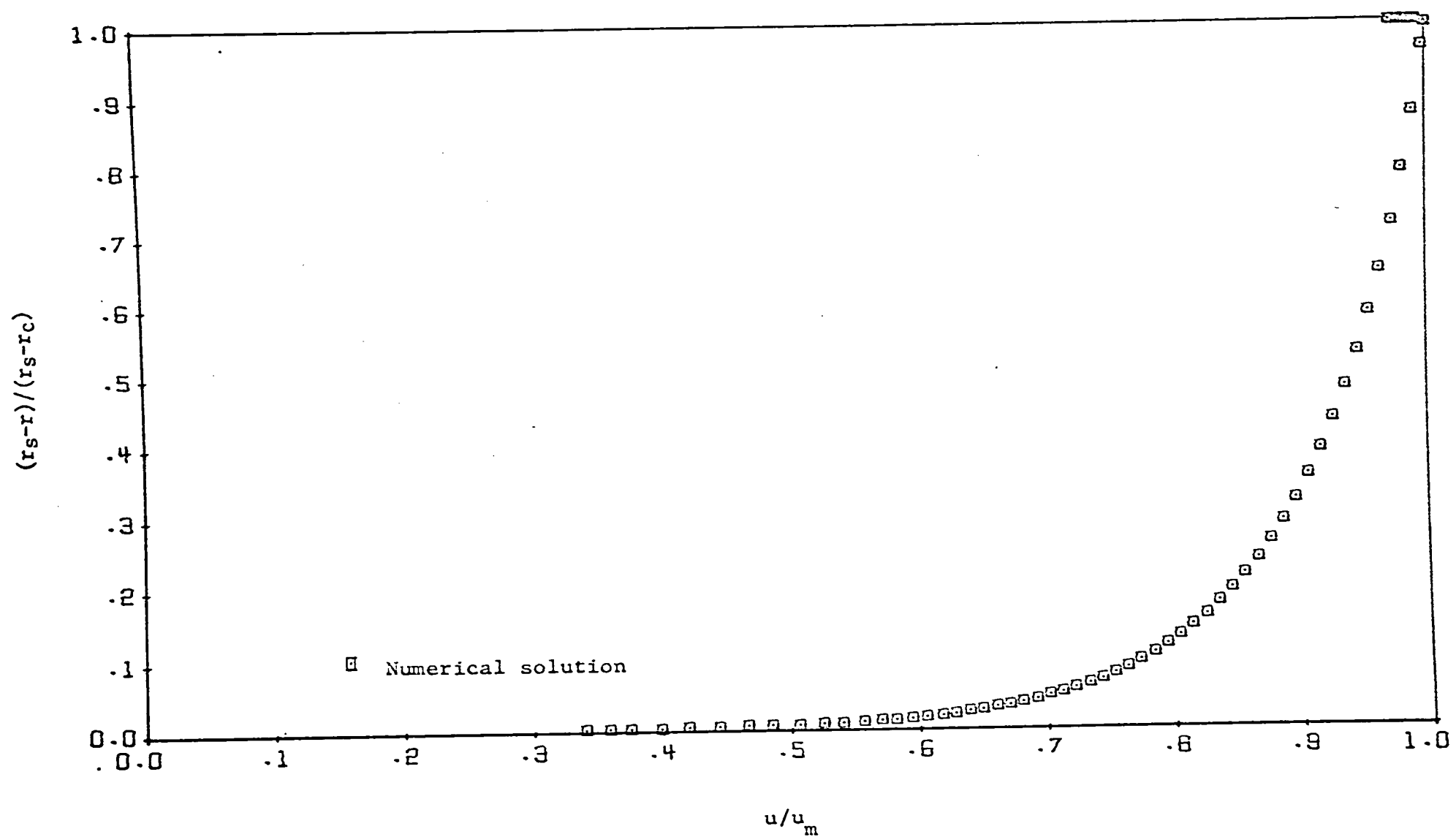


## FIGURE 25

MEAN VELOCITY PROFILE FOR AIR FLOWING IN AN ANNULUS  
WITH A CORE-TO-SHELL RATIO OF 0.0010 AT A MAXIMUM VELOCITY OF 60 FPS

Note: Eqn. 8 was used to locate the maximum velocity radius

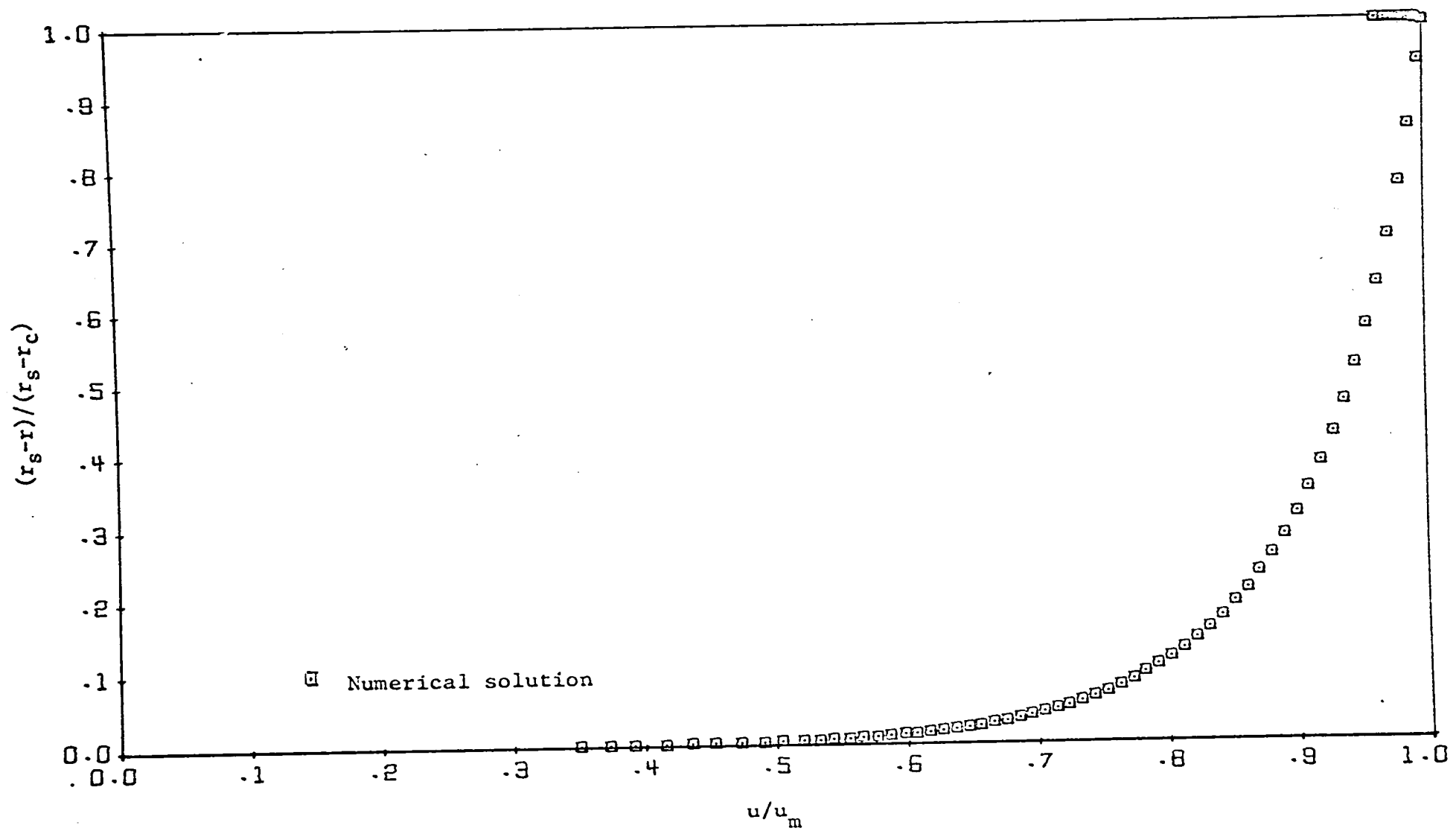


## FIGURE 26

MEAN VELOCITY PROFILE FOR AIR FLOWING IN AN ANNULUS  
WITH A CORE-TO-SHELL RATIO OF 0.9900 AT A MAXIMUM VELOCITY OF 30 FPS

Note: Eqn. 8 was used to locate the maximum velocity radius

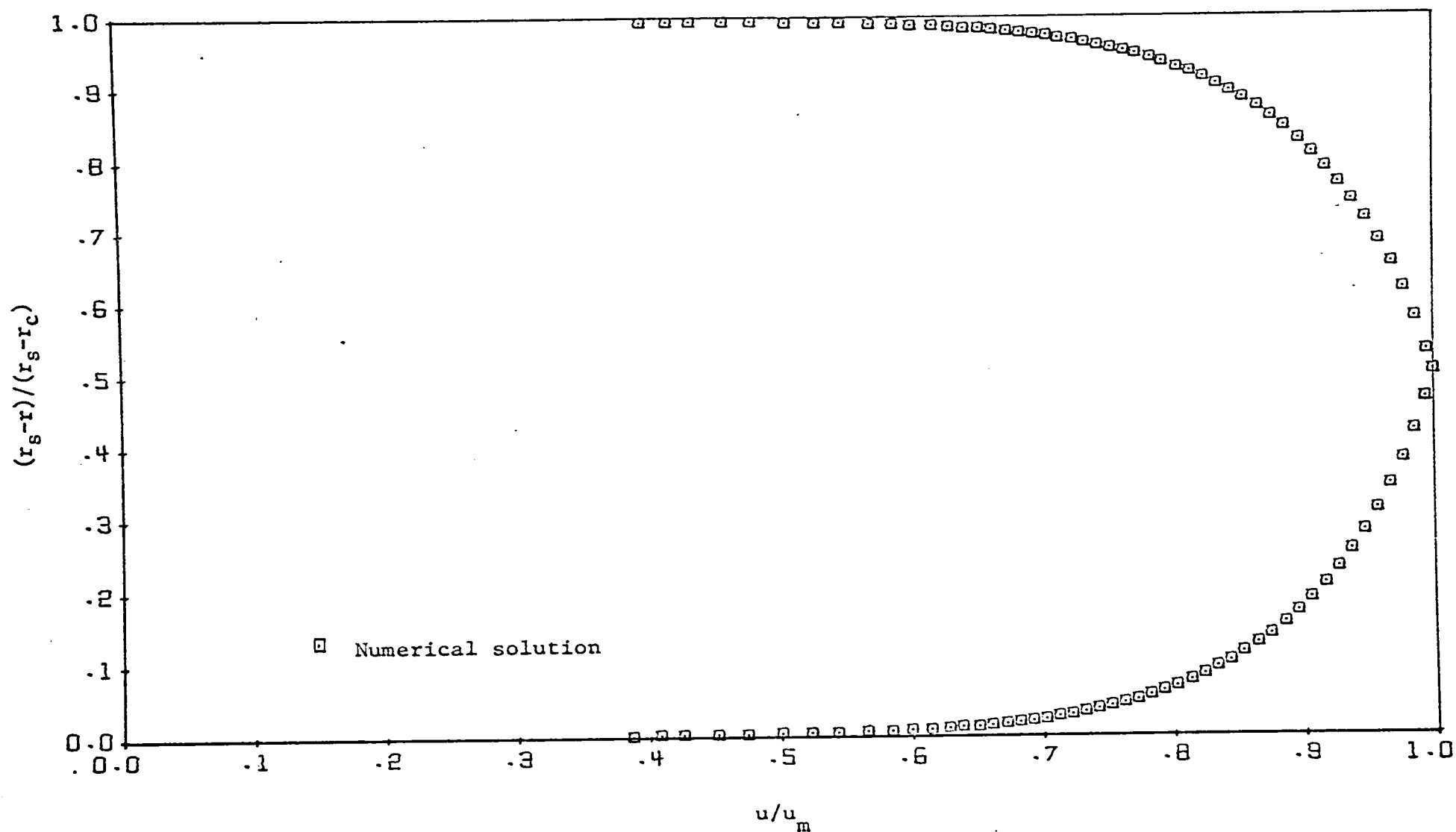
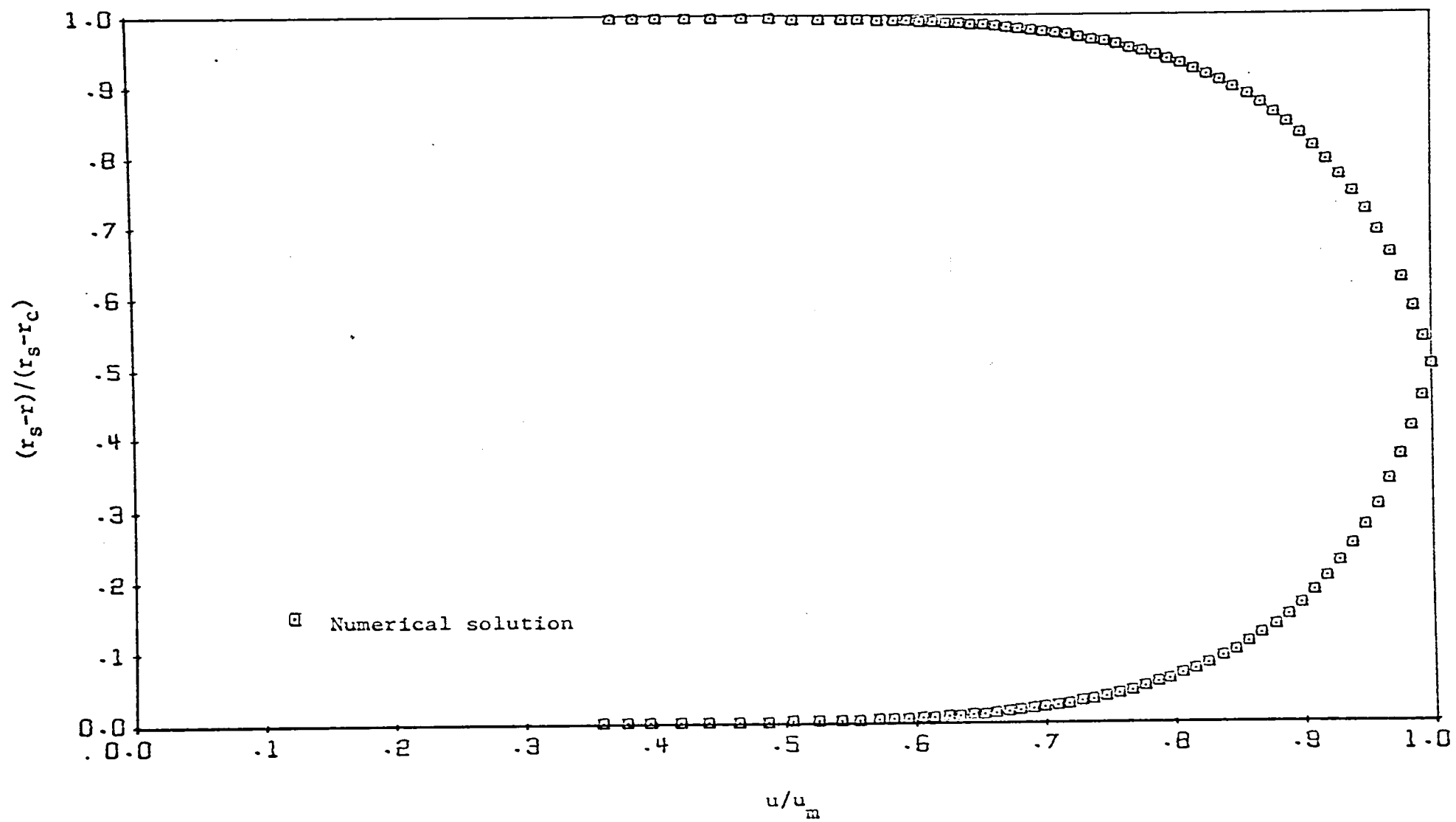


## FIGURE 27

MEAN VELOCITY PROFILE FOR AIR FLOWING IN AN ANNULUS  
WITH A CORE-TO-SHELL RATIO OF 0.9900 AT A MAXIMUM VELOCITY OF 60 FPS

Note: Eqn. 8 was used to locate the maximum velocity radius





APPENDICES

U+ Y+ TEST PROGRAM D. KWASNOSKI

SEPT 8, 1965

```

TEST PROGRAM NO. 2
DIMENSION SLOPE(2),UPLUS(3),YPLUS(2),FUJ(2,2),UDIST(2)
DIMENSION UMXZ(2)
FUJ(1,1)=2.
FUJ(1,2)=1.001
FUJ(2,1)=1.
FUJ(2,1)=2.
FUJ(2,2)=1.
FUJ(2,2)=1.001
UDIST(1)=0.
UDIST(2)=1.
READ 251, JY
251 FORMAT(15)
500 TYPE 98
98 FORMAT(58H ENTER DATA AND SET SENSE SWITCH 1 IF DESIRED, PRESS STA
1RT)
PAUSE
READ 1, UMXZ
READ 1, RADS,RADC,UMAX, DIF,DELT1,RATE0,EN1,EN2,EN3,EN4
1 FORMAT(3F10.4,F10.6,2F10.4,4F5.3)
RATIO=RADC/RADS
TYPE 1, RATIO,RATE0
IF(SENSE SWITCH 1) 100,200
200 RADM=RADS*SQRTF((1.-RATIO**2)/(2.*LOGF(1./RATIO)))
MNT=1
GO TO 300
100 IF(RATIO-.0624) 301,301,302
302 FACT=1.0754793*(RATIO**3)-2.2025076*(RATIO**2)+1.6523402*RATIO
1+.47504352
GO TO 303
301 FACT=.565*RATIO/.0624
303 RADM=FACT*(RADS-RADC)/2. +RADC
MNT=2
300 RADZ=(RADS-RADM)*100./(RADS-RADC)
UAVG=0.
DO 510 MZ=1,2
UAVG1=0.
YAVG1=0.
JOUNT=0
KOUNT=0
NNT=1
JY=JY+1
PUNCH 256, JY
256 FORMAT(1H1,35X,5HTABLE13)
JNT=1
UPLSM=UMXZ(MZ)
UAST=UMAX/UPLSM
GO TO(312,311),MZ
311 YPLSM=UAST*(RADM-RADC)/DIF
YMAX=RADM-RADC
GO TO 313
312 YPLSM=UAST*(RADS-RADM)/DIF

```

U+ Y+ TEST PROGRAM

D. KWASNOSKI

SEPT 8, 1965

```

YMAX=RADS-RADM
313 DO 610 NZ=1,10
    EM1=(RADS-RADC)/YMAX
    DELT=DELT1
    COUNT=0.
    NPLSM=YPLSM
    YPLSM=NPLSM
    TYPE 231, YPLSM,UPLSM,UMAX,UAST
    GO TO(315,314),JNT
315 GO TO(317,316),MZ
314 GO TO(212,211),MZ
211 PUNCH 40, RATEO
40 FORMAT(59H VELOCITY DISTRIBUTION FOR LAW OF WALL (INNER PROFILE),
    1S =F6.4)
    GO TO(255,257),MNT
255 PUNCH 259
259 FORMAT(63H MAXIMUM VELOCITY RADIUS = LAMINAR FLOW MAXIMUM VELOCITY
    1 RADIUS)
    GO TO 260
257 PUNCH 258
258 FORMAT(63H MAXIMUM VELOCITY RADIUS = EXPERIMENTAL MAXIMUM VELOCITY
    1 RADIUS)
260 PUNCH 231, YPLSM,UPLSM,UMAX,UAST
231 FORMAT(9H Y+ MAX =F8.1,11H, U+ MAX =F5.1,10H, U MAX =F6.1,7H, U
    1* =F6.2)
    PUNCH 55, RADZ
55 FORMAT(29H MAXIMUM VELOCITY RADIUS LIESF4.0,26H PERCENT IN FROM TH
    1E SHELL//)
    PUNCH 41
41 FORMAT(80H      LN Y+      U+      Y+      DU+/DY+      U
    1 Y      U/UMAX  Y2/((RS-RC)/)
    GO TO(316,811,813),NNT
316 C1=(RADM**2)*RADC/((RADM**2)-(RADC**2))
    C3=RADC
    C4=C1*DIF/UAST/(RADM**2)
    C5=C1*RADC/(RADM**2)
    SLOPE(1)=1.
    GO TO 221
212 PUNCH 220, RATEO
220 FORMAT(59H VELOCITY DISTRIBUTION FOR LAW OF WALL (OUTER PROFILE),
    1S =F6.4)
    GO TO(265,267),MNT
265 PUNCH 259
    GO TO 270
267 PUNCH 258
270 PUNCH 231, YPLSM,UPLSM,UMAX,UAST
    PUNCH 55, RADZ
    PUNCH 41
    GO TO(317,811,813),NNT
317 C1=(RADM**2)*RADS/((RADM**2)-(RADS**2))
    C1=-C1
    C3=-RADS

```

U+ Y+ TEST PROGRAM D. KWASNOSKI

SEPT 8, 1965

```

C4=C1*DIF/UASt/(RADM**2)
C5=C1*C3/(RADM**2)
SLOPE(1)=-1.
221 C2=DIF/UASt
C6=EN1**2
UPLUS(1)=0.
YPLUS(1)=0.
UPLUS(2)=UPLUS(1)+DELT*SLOPE(1)
YPLUS(2)=YPLUS(1)+DELT
103 SLOPE(2)=(C1/(YPLUS(2)*C2+C3) - (C4*YPLUS(2)) - C5)/
1(1.+C6*UPLUS(2)*YPLUS(2))
UPLUS(3)=UPLUS(1)+DELT*((SLOPE(1)+SLOPE(2))/2.)
TEST=ABSF(UPLUS(2)-UPLUS(3))
IF (TEST-.001) 106,106,105
105 UPLUS(2)=UPLUS(3)
GO TO 103
106 UPLUS(1)=UPLUS(3)
UPLSB=0.
YPLUS(1)=YPLUS(2)
SLOPE(1)=SLOPE(2)
YPLST=2.2
JJ=YPLSM/DELT
DO 10 J=1,JJ
C6=(EN1+(YPLUS(1)*EN4*EM1/26.))**2
COUNT=COUNT+1.
UPLUS(2)=UPLSB+DELT*2.*SLOPE(1)
YPLUS(2)=YPLUS(1)+DELT
UPLSB=UPLUS(1)
3 SLOPE(2)=(C1/(YPLUS(2)*C2+C3) - (C4*YPLUS(2)) - C5)/
1(1.+C6*UPLUS(2)*YPLUS(2))
UPLUS(3)=UPLUS(1)+DELT*((SLOPE(1)+SLOPE(2))/2.)
TEST=ABSF(UPLUS(2)-UPLUS(3))
IF (TEST-.001) 6,6,5
5 UPLUS(2)=UPLUS(3)
GO TO 3
6 UPLUS(1)=UPLUS(3)
YPLUS(1)=YPLUS(2)
SLOPE(1)=SLOPE(2)
GO TO(202,341),JNT
341 YPLSL=LOGF(YPLUS(1))
IF (YPLSL-YPLST-.1) 202,201,201
201 UREG=UPLUS(1)*UASt
YREG=YPLUS(1)*DIF/UASt
UREG1=UREG/UMAX
YREG1=UDIST(MZ)-YREG/(RADS-RADC)
YREG1=ABSF(YREG1)
IF (KOUNT-48) 811,811,812
812 NNT=2
KOUNT=0
PUNCH 887, JY
GO TO(212,211),MZ
811 PUNCH 9, YPLSL,UPLUS(1),YPLUS(1),SLOPE(1),UREG,YREG,UREG1,YREG1

```

SEPT 8, 1965

U+ Y+ TEST PROGRAM D. KWASNOSKI

```

UAVG1=(UAVG1+UREG)/2.
YAVG1=(YREG-YAVG1)
UAVG=UAVG+UAVG1*YAVG1
UAVG1=UREG
YAVG1=YREG
KOUNT=KOUNT+1
JOUNT=JOUNT+1
YPLST=YPLST+.1
9 FORMAT(F10.4,2F10.3,F10.4,F10.3,F10.4,F8.4,2XF8.4)
202 IF(YPLUS(1)-YPLSM) 304,560,560
304 IF(YPLUS(1)-26.) 10,11,11
10 CONTINUE
11 DO 20 J=1,JJ
COUNT=COUNT+1.
IF(J-150) 711,708,981
708 DELT=DELT*FUJ(JNT,1)
GO TO 711
981 DELT=DELT*FUJ(JNT,2)
711 C6=EN2+(26.*EN3*EM1/YPLUS(1))
TEST1=C1/(C2*YPLUS(1)+C3)-C4*YPLUS(1)-C5
TRY1=-DELT*C6*SLOPE(1)**2/(SQRTF(TEST1-SLOPE(1)))
TEST1=C1/(C2*(YPLUS(1)+DELT/2.)+C3)-C4*(YPLUS(1)+DELT/2.)-C5
TRY2=-DELT*C6*(SLOPE(1)+TRY1/2.)*(SLOPE(1)+TRY1/2.)/
1(SQRTF(TEST1-SLOPE(1)-TRY1/2.))
TRY3=-DELT*C6*(SLOPE(1)+TRY2/2.)*(SLOPE(1)+TRY2/2.)/
1(SQRTF(TEST1-SLOPE(1)-TRY2/2.))
TEST1=C1/(C2*(YPLUS(1)+DELT)+C3)-C4*(YPLUS(1)+DELT)-C5
TRY4=-DELT*C6*(SLOPE(1)+TRY3)*(SLOPE(1)+TRY3)/
1(SQRTF(TEST1-SLOPE(1)-TRY3))
UPLUS(1)=UPLUS(1)+DELT*(SLOPE(1)+(1./6.)*(TRY1+TRY2+TRY3))
SLOPE(1)=SLOPE(1)+(1./6.)*(TRY1+TRY2*2.+TRY3*2.+TRY4)
YPLUS(1)=YPLUS(1)+DELT
IF(YPLUS(1)-YPLSM+50.) 30,30,560
30 GO TO(20,351),JNT
351 YPLSL=LOGF(YPLUS(1))
IF(YPLSL-YPLST-.1) 20,204,204
204 UREG=UPLUS(1)*UAST
YREG=YPLUS(1)*DIF/UAST
UREG1=UREG/UMAX
YREG1=UDIST(MZ)-YREG/(RADS-RADC)
YREG1=ABSF(YREG1)
IF(KOUNT-48) 813,813,814
814 NNT=3
KOUNT=0
PUNCH 887, JY
887 FORMAT(1H1,35X,5HTABLE13,8H (CONT.))
GO TO(212,211),MZ
813 PUNCH 9, YPLSL,UPLUS(1),YPLUS(1),SLOPE(1),UREG,YREG,UREG1,YREG1
UAVG1=(UAVG1+UREG)/2.
YAVG1=(YREG-YAVG1)
UAVG=UAVG+UAVG1*YAVG1
UAVG1=UREG

```

U+ Y+ TEST PROGRAM

D. KWASNOSKI

SEPT 8, 1965

```

YAVG1=YREG
KOUNT=KOUNT+1
JOUNT=JOUNT+1
YPLST=YPLST+.1
20 CONTINUE
560 UPLSN=UPLUS(1)+SLOPE(1)*(YPLSM-YPLUS(1))
    TYPE 1, DELT
    TYPE 777, COUNT
777 FORMAT(F10.0)
    GO TO(562,561),JNT
561 YPLSL=LOGF(YPLSM)
    UREG1=1.
    YREG1=UDIST(MZ)-(YMAX/(RADS-RADC))
    YREG1=ABSF(YREG1)
    PUNCH 9, YPLSL,UPLSN,YPLSM,SLOPE(1),UMAX,YMAX,UREG1,YREG1
    UREG=UMAX
    YREG=YMAX
    UAVG1=(UAVG1+UREG)/2.
    YAVG1=(YREG-YAVG1)
    UAVG=UAVG+UAVG1*YAVG1
    UAVG1=UREG
    YAVG1=YREG
    JOUNT=JOUNT+1
    PUNCH 888, JOUNT
888 FORMAT(/33H NUMBER OF POINTS IN THIS GROUP =14)
    GO TO 510
562 IF(NZ-9) 563,564,1000
563 TEST=ABSF(UPLSN-UPLSM)
    IF(TEST-.5) 564,564,565
564 JNT=2
565 UPLSM=.90*UPLSN+.10*UPLSM
    UAST=UMAX/UPLSM
    YPLSM=UAST*YMAX/DIF
610 CONTINUE
510 CONTINUE
    UAVG=UAVG/(RADS-RADC)
    VAVG=UAVG/UMAX
    PUNCH 881,UAVG,VAVG
881 FORMAT(19H AVERAGE VELOCITY =F7.2,23H AVG TO MAX VEL RATIO =F5.3)
    GO TO 500
1000 END

```

DATA FOR U+ Y+ TEST PROGRAM D KWASNOSKI

SEPT 08, 1965

0  
 25.0000 15.0000  
 .3333 .0208 30.0000 .000166 .5000 .0625 .109 .360 .200 .01

THE ABOVE DATA HAVE THE FOLLOWING SIGNIFICANCE

## FIRST CARD

NUMBER OF THE LAST DATA SET STUDIED = 0

## SECOND CARD

ESTIMATED MAXIMUM VALUE OF U+ FOR THE OUTER REGION = 25.0000  
 ESTIMATED MAXIMUM VALUE OF U+ FOR THE INNER REGION = 15.0000

## THIRD CARD

RADIUS OF THE SHELL OF THE ANNULUS = .3333  
 RADIUS OF THE CORE OF THE ANNULUS = .0208  
 MAXIMUM VELOCITY IN THE ANNULUS = 60.0000  
 KINEMATIC VISCOSITY OF AIR = .000166  
 INCREMENT SIZE USED IN THE NUMERICAL INTEGRATIONS = .5000  
 RATIO OF THE CORE RADIUS TO THE SHELL RADIUS = .0625  
 THE CONSTANT F IN EQNS. 25 AND 26 = .109  
 THE CONSTANT F IN EQNS. 25A AND 25B = .109  
 THE CONSTANT H IN EQNS. 26A AND 26B = .360  
 THE CONSTANT J IN EQNS. 26A AND 26B = .200

BIBLIOGRAPHY

1. Batchelor, G. K., "Note on Free Turbulent Flows With Special Reference to the Two-Dimensional Wake," Journal of the Aeronautical Sciences, Vol. 17 (1950), pp. 441-445.
2. Bird, R. B., Stewart, W. E., and Lightfoot, E. N., Transport Phenomena, John Wiley and Sons, Inc., New York, (1962).
3. Brighton, J. A., and Jones, J. B., "Fully Developed Turbulent Flow in Annuli," Journal of Basic Engineering, (1964), pp. 835-844.
4. Clauser, F. H., "Turbulent Boundary Layers in Adverse Pressure Gradients," Journal of the Aeronautical Sciences, Vol. 21 (1954), pp. 91-108.
5. Deissler, R. G., "Analytical and Experimental Investigation of Adiabatic Turbulent Flow in Smooth Tubes," U.S. National Advisory Committee for Aeronautics, Technical Note 2138, (1950).
6. Deissler, R. G., "Analysis of Turbulent Heat Transfer Mass Transfer and Friction in Smooth Tubes at High Prandtl and Schmidt Numbers," NACA TN3145, (1954).
7. Eskinazi, S., and Yeh, H., "An Investigation on Fully Developed Turbulent Flows in a Curved Channel," Journal of Aeronautical Sciences, Vol. 23 (1956), pp. 23-34, 75.
8. Fredrickson, A. G., and Bird, R. B., "Friction Factors in Non-Newtonian Annular Flow," Industrial and Engineering Chemistry, Vol. 50 (1958), p. 1599.
9. Hinze, J. O., Turbulence, McGraw-Hill, New York, (1959).
10. Hinze, J. O., "Turbulent Pipe Flow," Chapter in The Mechanics of Turbulence, International Symposium of the National Scientific Research Center, August 28 to September 1, 1961, Gordon and Breach, New York, (1964).



11. Knudsen, J. G., and Katz, D. L., "Velocity Profiles in Annuli," Proceedings of the Midwestern Conference of Fluid Dynamics, (1950), pp. 175-203.
12. Knudsen, J. G., and Katz, D. L., Fluid Dynamics and Heat Transfer, McGraw-Hill, New York, (1958).
13. Laufer, J., "Investigation of Turbulent Flow in a Two-Dimensional Channel," NACA Report 1053, (1951).
14. Laufer, J., "The Structure of Turbulence in Fully Developed Pipe Flow," NACA Report 1174, (1954).
15. Millikan, C. B., "Critical Discussion of Turbulent Flows in Channels and Circular Tubes," Proceedings of the Fifth International Congress for Applied Mechanics, (1938).
16. Okiishi, T. H., and Serovy, G. K., "Experimental Velocity Profiles for Fully Developed Turbulent Flow of Air in Concentric Annuli," Publication of The American Society of Mechanical Engineers, No. 64-WA/FE-32, (1964).
17. Rannie, W. D., "Heat Transfer in Turbulent Shear Flow," Journal of the Aeronautical Sciences, Vol. 23, (1956), pp. 485-489.
18. Ratkowsky, D. A., "Fluid Friction and Heat Transfer in Plain, Concentric Annuli," Journal of Canadian Chemical Engineering, (1966), pp. 8-12.
19. Rothfus, R. R., "Velocity Gradients and Friction in Concentric Annuli," Unpublished Ph.D. thesis, Library, Carnegie Institute of Technology, Pittsburgh, Pennsylvania, (1948).
20. Sandborn, V. A., "Experimental Evaluation of Momentum Terms in Turbulent Pipe Flow," NACA TN3266, (1955).
21. Scarborough, J. B., Numerical Mathematical Analysis, Fifth Edition, The Johns Hopkins Press, (1962).

22. Seagrave, R. C., "The Distributions of Eddy Viscosity and Turbulent Velocity in Pipe Flow," Journal of The American Institute of Chemical Engineers, (1965), pp. 745, 749, 759.
23. Spalding, D. B., "A Single Formula for the Law of the Wall," Journal of Applied Mechanics, Vol. 28 (1961), pp. 455-457.
24. Sparrow, E. H., Eckert, E. R. G., and Minkowycz, W. J., "Heat Transfer and Skin Friction for Turbulent Boundary Layer Flow Longitudinal to a Circular Cylinder," Journal of Applied Mechanics, Vol. 42 (1963), p. 37.
25. Th. von Karman, "The Analogy Between Fluid Friction and Heat Transfer," Trans. American Society of Mechanical Engineers, Vol. 61 (1939), pp. 705-710.
26. Walker, J. E., Whan, G. A., and Rothfus, R. R., "Fluid Friction in Noncircular Ducts," Journal of The American Institute of Chemical Engineers, Vol. 3 (1957), pp. 484-489.
27. Wang, C. T., "On the Velocity Distribution of Turbulent Flow in Pipes and Channels of Constant Cross Section," Journal of Applied Mechanics, Vol. 68 (1946), pp. A85-A90.
28. Wolffe, R. A., Personal Interview, July, (1965).
29. Wolffe, R. A., "Development of Universal Velocity Distribution Laws for Turbulent Flows in Which Shear Stress is a Nonlinear Function of Distance from the Wall," Unpublished proposal presented in partial fulfillment of the requirements for Ph.D., Lehigh University, Bethlehem, Pennsylvania, (1965).

VITA

The author was born on December 12, 1934, the son of Michael J. and Eva Kwasnoski. While a resident of Ranshaw, Pennsylvania, he attended Coal Township High School, graduating in 1952. The next three years were spent in the employ of J. J. Newberry Company as a stockman and department manager. In 1955 a two-year tour of duty with the U. S. Army was undertaken, sixteen months of which were spent in Hanau, Germany.

In 1957 he resumed his formal education, spending four years at the Pennsylvania State University where he received a Bachelor of Science degree in chemical engineering in 1961. In that same year he married Carolyn A. McCall, and joined the Bethlehem Steel Corporation as a member of that year's management training program. Since that time he has been employed at the Homer Research Laboratories of the Bethlehem Steel Corporation, Bethlehem, Pennsylvania as an Engineer-assistant and Research engineer.